Computer Communications 149 (2020) 146–161

Contents lists available at ScienceDirect

Computer Communications

journal homepage: www.elsevier.com/locate/comcom

Efficient dynamic relay probing and concurrent backhaul link scheduling for mmWave cellular networks

Anup Chaudhari *, C. Siva Ram Murthy

Department of Computer Science and Engineering, Indian Institute of Technology Madras, 600036, India

ARTICLE INFO

Keywords:
mmWave
5G cellular network
FBS-to-FBS (F2F) communication
Mode selection
Relay probing
Backhaul link scheduling

ABSTRACT

Exploiting the enormous chunks of mmWave spectrum between 30 GHz and 300 GHz have the potential to facilitate gigabit rate services to the future 5G cellular networks, and help in alleviating the current spectrum crisis. Conventional backhaul links such as Digital Subscriber Line (DSL) and Asymmetric Digital Subscriber Line (ADSL) have been proved to be a major bottleneck in satisfying these high data rate demands of indoor user equipments associated with traditional Femto Base Stations (FBS). One possible solution is to deploy higher capacity optical fiber cable to satisfy such demands. However, it is a costly and non-flexible solution. Thus, mmWave wireless backhaul links can be utilized at the FBSs. But due to their high-frequency, mmWave carrier signals are highly susceptible to obstacles and thus suffer a high attenuation in signal strength when passed through the obstacles. In order to alleviate the losses incurred due to blockages and to improve the signal reachability, in this paper, we propose an efficient distributed mode selection and dynamic relay probing scheme. We also propose an efficient scheduling scheme, for scheduling wireless backhaul links, which works jointly with the proposed mode selection and relay probing scheme to further improve the system throughput. Our proposed scheduling scheme permits non-interfering links to schedule and transmit concurrently. An expression for calculating the expected number of concurrent transmissions for our proposed scheduling scheme is derived and validated. Through extensive simulations under various system parameters, we have demonstrated the superiority of our proposed mode selection and relay probing scheme over the fixed relay probing scheme.

1. Introduction

The exponential growth in wireless services because of billions of devices, users, and connections have driven the need for a transition from 4G to 5G cellular network standards. Standards for the 5G cellular networks deployment have not been finalized till date. However, by considering the business and the consumer demands Next Generation Mobile Networks (NGMN) Alliance forecasted that the first phase of 5G networks should be deployed by 2020 [1]. The NGMN Alliance has also outlined a few important requirements that 5G cellular network standards should meet. These requirements include:

- High data rates of tens of Mbps for tens of thousands of users.
- Simultaneously multi-gigabit data rates to many workers on the same office floor.
- Data rates of 100 Mbps for metropolitan areas.
- Several hundreds of thousands of concurrent connections for wireless sensors.
- Better coverage, improved spectral efficiency, and significantly low latency as compared to Long Term Evolution (LTE).

The unprecedented growth in the number of cellular broadband users and data-intensive applications (high definition video streaming, ultra-fast file transfer, augmented reality, and virtual reality games, etc.) resulted in multi-gigabit rate requirements [2]. However, most of the data traffic because of these applications is generated by in-door User Equipments (UEs) associated with low powered Femto Base Stations (FBSs) [3]. In order to satisfy the data rate requirements, the radio access (FBS-UE) link capacity can be increased with the help of millimeter Wave (mmWave) techniques, higher cellular spectrum reuse, and unlicensed carrier aggregation. On the other hand, in order to carry the indoor aggregated data traffic because of the new data-intensive applications, traditional broadband connection based backhaul (such as Digital Subscriber Line (DSL) and Asymmetric Digital Subscriber Line (ADSL)) cannot be used. The traditional broadband-based connection can provide data rates up to tens of Mbps only and can become a bottleneck [4]. One possible solution in order to satisfy the backhaul requirements can be the use of optical fiber links. However, in order to cater to exponentially increasing users and their requirements, a dense deployment of FBSs is required [5]. Connecting FBSs to the other FBSs and to the Micro Base Station (MiBS) by optical fiber cable will

* Corresponding author.
E-mail addresses: anup.chaudhari93@gmail.com (A. Chaudhari), murthy@iitm.ac.in (C.S.R. Murthy).

https://doi.org/10.1016/j.comcom.2019.09.019
Received 28 May 2019; Received in revised form 19 September 2019; Accepted 25 September 2019
Available online 4 October 2019

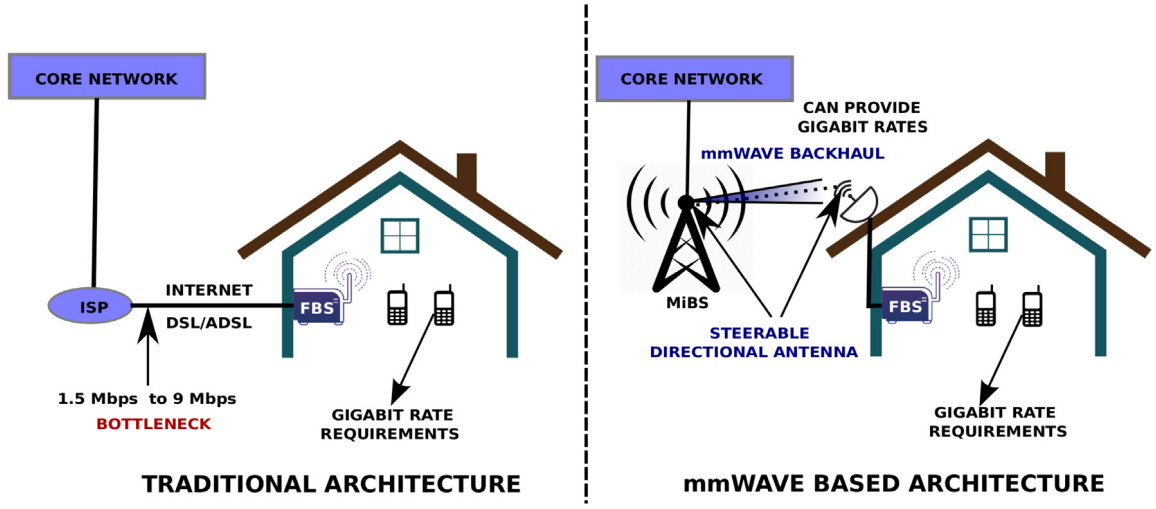

Fig. 1. Traditional architecture vs. mmWave based architecture.

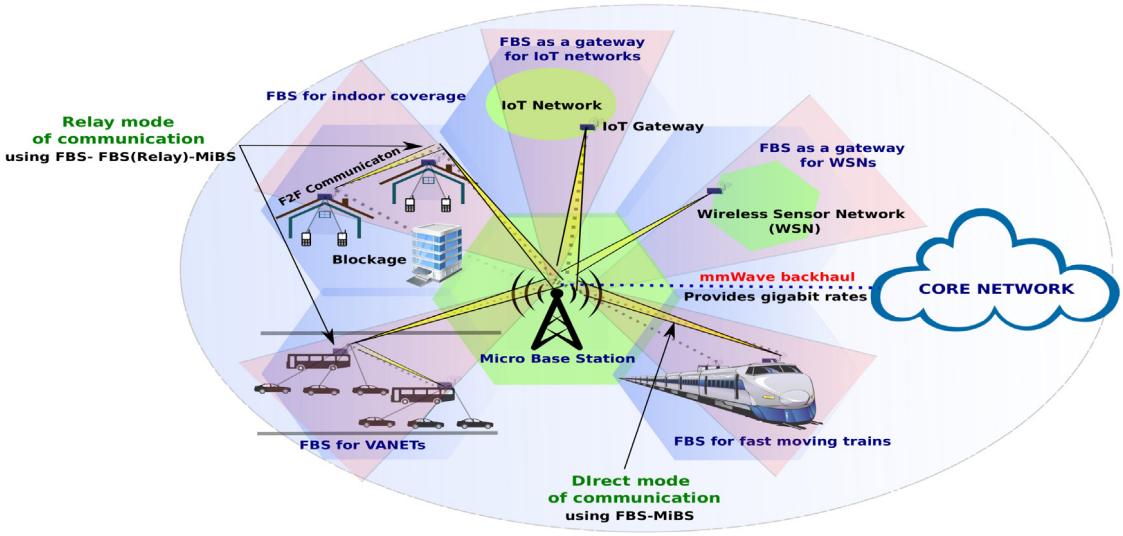

Fig. 2. Future use cases of mmWave communication exploiting F2F communication.

increase the deployment and maintenance cost. Thus, mmWave based wireless backhaul at FBS can be a good solution compared to traditional broadband connections and optical fiber cables. A large amount of free bandwidth available at mmWave band is capable of solving the bottleneck issue. Wireless mmWave based backhaul not only fulfills the data rate requirements but is also cost-effective, flexible, and easy to deploy as compared to optical fiber backhaul links. Benefits of using mmWave based backhaul at FBSs is well discussed in our previous work [6]. Fig. 1 shows the comparison between traditional DSL and ADSL based backhaul architecture and mmWave based backhaul architecture.

In some of the future use cases, wireless backhaul is the only possible solution because of mobility of FBSs. For example, big vehicles (buses, trucks, etc.) supported by FBSs can provide better connectivity to other small fast moving autonomous vehicles in VANETs (Vehicular Ad Hoc Networks) [7], fast-moving trains supported by FBSs provide connectivity to passengers [8], etc. Fig. 2 shows various application scenarios where FBS-to-FBS (F2F) communication can be beneficial. It also shows usage of two modes of communication, viz. direct and relay. Huge chunks of bandwidth available in the mmWave frequency band (30–300 GHz) can be utilized to satisfy the backhaul links' rate requirements of future 5G cellular networks [9–12]. mmWave 60 GHz band, E-band (71–76 GHz and 81–86 GHz), etc. have the capabilities to satisfy these rate requirements, and can be promising backhaul solutions to meet the data rate demands of future cellular networks. Motivated by all these facts, we consider mmWave wireless backhaul links between FBSs, and also between an FBS and MiBS.

mmWave signals suffer from high free space path loss, considerable oxygen absorption, and attenuation due to blockages. For example, mmWave signals get attenuated from 20 dB to 35 dB when passed through human body [13]. Hence, both MiBS and FBSs are expected to be equipped with directional antennas that will help in achieving high data rate and longer transmission range. However, direct communication between FBS-MiBS may not always provide required data rate because of the unusual characteristics of mmWave (for example, large building blockages coming in between FBSs and MiBS). One promising strategy to get rid of signal losses due to blockages is to employ relays. Any FBS can act as a relay which is not performing any data transmission. Relays can provide an alternative multi-hop path, and increase the probability of signals to reach the receiver (MiBS). Thus, relays help in increasing the system throughput thereby increasing backhaul flows (single hop or multi-hop paths) throughput.

Though relays can provide an alternative multi-hop path for signals to reach the destination, determining whether a relay is appropriate or not needs learning of both source–relay (i.e., FBS-FBS (Relay)) and relay–destination (i.e., FBS (Relay)-MiBS) channels. For channel

estimation, mmWave transmitter and receiver need to align their antenna beam towards each other and this beam alignment takes a non-negligible overhead. In this paper, we call *probing* as the process of exploring whether a particular transmitter and receiver pair can provide a required link capacity or not, after performing beam alignment. Hence, probing more relays may increase the probability of finding a better relay but at the cost of more probing overhead. Thus, there is a tradeoff in searching for a good relay in mmWave systems. Hence, in order to maximize the backhaul flow throughput, proper mode selection is important. It is also essential to determine how many relays should be probed in mmWave systems or in other words it is important to determine a bound on the number of probes. Our paper addresses these issues and determines the bound on the number of probes.

In this paper when we say probe it means probing single transmitter and receiver pair. Hence, probing FBS-FBS (Relay) and FBS (Relay)-MiBS requires two independent probes.

Most of the current research studies on FBSs were done using the sub-6-GHz band. Chen et al. [14] have proposed backhaul-constrained resource optimization for distributed femtocell interference mitigation. An energy efficient cell selection framework for femtocell networks with limited backhaul link capacity is proposed in [15]. Chu et al. [4] have discussed backhaul-constrained cooperative management strategy for interference management in dense femtocell networks. These studies consider backhaul-constrained resource allocation or interference management because of limited backhaul capacity of broadband connection such as ADSL.

The existing relaying and link scheduling techniques for 4G cellular networks are designed considering omnidirectional antennas, which may be sub-optimal for mmWave 5G cellular networks. This is due to the different channel characteristics and usage of directional antennas in mmWave communication as compared to 4G LTE.

The existing research work on mmWave transmission and link scheduling is mostly focused on Wireless Personal Area Network (WPAN) [16], Wireless Local Area Network (WLAN) [17], and ECMA-387 [18]. Cai et al. [19] have derived the exclusive region conditions and used these conditions for concurrently scheduling the links efficiently in Wireless Personal Area Network (WPAN). The derived conditions ensure better performance than Time Division Multiple Access (TDMA). In the protocols proposed in [20,21] for WPAN, multiple links are concurrently scheduled to communicate in the same slot if the interference due to multiple links is below a specific threshold. Rehman et al. [22] have considered an ideal directional antenna and proposed a vertex multiple coloring concurrent transmission scheme for Device-to-Device (D2D) network over unlicensed 60 GHz mmWave band. They have also proposed that while scheduling different flows, preference should be given to the flows having better chances for higher data rate. Spatial-time division multiple-access scheduling algorithm for WPAN considering the mmWave band has been studied in [23]. The algorithm allows both interfering and non-interfering links to transmit concurrently while satisfying the Quality of Service (QoS) requirements of each link. He et al. [24] have developed a decomposition principle in order to minimize the maximum expected delivery time for the link and relay selection in centralized dual-hop 60 GHz networks. Qiao et al. [25] have addressed a resource sharing scheme by allowing non-interfering D2D links to operate concurrently in an mmWave 5G cellular network.

Gia Khanh Tran et al. [26] have proposed a method to control mmWave meshed backhaul for efficient operation of mmWave overlay 5G HetNet through Software-Defined Network (SDN) technology. Their proposed method is featured by two functionalities, i.e., backhauling route multiplexing for overloaded mmWave small cell base stations (SC-BSs) and mmWave SC-BSs' ON/OFF status switching for an underloaded spot. They assume backhaul interfaces of SC-BSs are located at the streets lamp posts and Line-of-Sight (LOS) conditions are always guaranteed. However, in practical scenarios it might not be true. H. Ogawa et al. [27] have proposed a traffic-adaptive formation for outdoor hotspots. They have proposed a load balancing mechanism called route multiplexing to support certain mmWave APs which need to accommodate traffic higher than what their mmWave gateway (GW) sectors can support. Especially, the architecture employs multi-hop relay to support mmWave APs located far from the GW. The proposed mechanism assumes zero interference among backhaul links. However, in practical deployment scenarios, interference among backhaul links cannot be ignored as it will create network bottleneck and affects the whole system rate. A. Mesodiakaki et al. [28] propose an optimization framework for the design of policies that help in solving the problem of where to associate a user, subsequent routing of packets over the backhaul, and identifying which backhaul links and base stations to be switched off such that energy cost is minimized without hampering the user demands. They assume LOS conditions are always guaranteed between mmWave backhaul links. Also, they consider the interference among adjacent backhaul links is negligible.

To the best of our knowledge, no work in the literature focuses on the scheduling of mmWave based backhaul for FBSs by jointly considering the mode selection and relay probing costs. The mmWave band can provide the required capacity, but proper scheduling of mmWave based backhaul link for FBS is very important in order to achieve the maximum benefit. Our paper targets the same as one of the major objectives.

One of the promising works for relay probing in mmWave cellular networks is proposed in [29] for D2D relaying. It was shown that throughput-optimal relay probing strategy is a pure threshold policy and relay probing can certainly be stopped once the optimized spectral efficiency threshold is achieved by a two-hop link. However, they have considered a single user scenario and left the multiuser scenario for future work. Apart from this, they have considered a full signal loss due to blockages, i.e., they consider received signal strength to be zero when an obstacle is present in between the transmitter and receiver, which might not capture the actual system scenario. Rebato et al. [30] have compared and examined several resource sharing configurations in 5G cellular networks in order to achieve the enhanced potential of mmWave communication. They have shown the advantage of full infrastructure and spectrum sharing configuration in terms of increase in user data rate, and economical advantages for each of the service providers. The problem of joint beamwidth selection and power control is well studied in [31]. Authors have shown the tradeoff between the beam alignment and throughput. They have proposed standard compliant algorithms for short wave mmWave scenarios considering the alignment-throughput tradeoff. However, they have left the extension of proposed work for the mmWave based cellular networks as a future work. Our work well studies the future work insights and intricacies of [29] and [31] considering cellular networks.

The existing research work has been mainly focused on mode selection, relay selection, and link scheduling in WPAN, WLAN, ECMA-387, etc. using mmWave spectrum or FBSs using broadband connection based backhaul. In contrast, our work particularly focuses on mode selection, relay probing, and efficient concurrent backhaul scheduling for FBSs using mmWave based backhaul. The main contributions of this paper are summarized as follows:

1. There exists a non-negligible beam-alignment overhead in mmWave systems because of the use of directional antennas. We consider a more practical and realistic scenario in scheduling the backhaul links for FBSs by explicitly considering the overhead incurred due to beam alignment.
2. Proper mode selection (direct or relay) of data transfer is important in order to maximize the system throughput. Our proposed solution efficiently determines the mode of data transfer and the best relay in case relay mode is selected.

3. Probing more relays may increase the chances of finding the better relay but at a cost of more probing overhead because of beam alignment. We identify the tradeoff between relay probing and throughput for a single FBS scenario and provide a heuristic for multiple FBSs scenario.
4. mmWave band has huge chunks of bandwidth available in order to cater FBS backhaul requirements. However, proper scheduling of backhaul links or flows is important. We propose an efficient polynomial time scheduling scheme which schedules non-interfering backhaul links concurrently.
5. We derive an expression for calculating the expected number of concurrent transmissions for our proposed scheduling scheme and validate it using extensive simulations.

In this work, we consider the maximum of two-hop communication links only because further increasing the hops may increase the delay and thereby reduce the system throughput. Also, it increases the overhead due to beam-searching overhead at each step in mmWave systems.

The paper is organized as follows. In Section 2, we explain system model for mmWave communication in cellular networks. Section 3 discusses the optimization problems for determining best stopping rule criteria and to maximize the number of concurrent backhaul link transmissions. Then, we discuss our proposed solutions for both the optimization problems in Section 4 by deriving various heuristics. In Section 5, we derive an expression for calculating the expected number of concurrent transmissions for our proposed concurrent backhaul link scheduling scheme. Section 6 presents the simulation and analytical results, and comparison with other schemes. Finally, conclusions are drawn in Section 7.

2. System model

Our network model consists of a single cell with an MiBS providing coverage to F active FBSs and $|Y|$ idle FBSs. Idle FBSs are the FBSs that are not involved in any kind of data transmissions and thus can act as relays. The transmission range of MiBS is considered to be R_ψ. The MiBS's entire coverage is divided into S $(= \frac{2\pi}{\theta'})$ sectors of equal beamwidth, where, θ' represents the beamwidth of a directional antenna of MiBS. Each FBS is served by the directional antenna of the sector in which it is present. Directional antennas of the MiBS have an ability to perform either concurrent transmission or concurrent reception without interfering with other ongoing transmissions. All the FBSs are considered to be employed with an electronically steerable directional antenna for transmitting and receiving the data and control information. We assume that all FBSs (whether FBS or FBS (Relay)) transmit with maximum transmit power P_t.

Relays are searched by FBSs when direct mode of data transfer (i.e., FBS-MiBS) is unable to provide the sufficient backhaul flow throughput (bits/sec). In this paper, the data from an FBS to the MiBS is sent either via a single hop or multi-hop path defined as a flow. We consider the overhead of beam-searching in our work. We also consider two different modes of data transmissions, viz. direct and relay. All the FBSs are assumed to be operating in half-duplex mode. We intend to minimize the interference among the different flows. Hence, we schedule only non-interfering flows concurrently in our work. We assume that the MiBS has a global knowledge of network topology, for example, location of FBSs, number of active links, etc. mmWave backhaul transceiver is kept at the rooftop and has a wired connectivity to the indoor FBS in order to maximize the probability of LOS between MiBS and FBS as shown in Fig. 1. In this paper, we examine the uplink data transmission system behavior only. However, the downlink scenario is exactly the opposite of the uplink scenario. In the case of downlink, the direction of the data traffic is from MiBS to FBS.

2.1. Antenna model

A high gain directional antenna is used in mmWave communication to overcome the atmospheric attenuation and the path loss incurred because of extremely high frequency. Both the transmitter and receiver use electronically steerable antenna arrays to achieve maximum transmission rates. Each antenna array consists of numerous small antenna elements that make it feasible to incorporate in devices to achieve directionality. Transmitter/Receiver uses beamforming techniques to direct its beam in the required direction [32]. The given system has been modeled using cone plus circular model [33]. Let g_m and g_s denote the antenna gains due to the main lobe and side lobe of transmitter/receiver, respectively and are given as follows:

$$g_m = \frac{2\pi}{\theta}\eta \tag{1}$$

$$g_s = \frac{2\pi}{2\pi - \theta}(1-\eta) \tag{2}$$

where, η is the radiation efficiency and θ is the beamwidth. We assume that MiBS and FBSs have the same beamwidth (i.e. $\theta' = \theta$). The transmit pattern of a directional antenna comprises of the main lobe and a set of side lobes. The main lobe contains the maximum transmit power whereas side lobes are smaller beams that contain the remaining energy and are drawn in all directions except that of the main lobe. Total antenna gain $g^t g^r$ of the received signal depends upon the alignment of lobes of directional antennas and is given by:

$$g^t g^r = \begin{cases} g_m^t g_m^r, & main - main\ lobe\ alignment \\ g_m^t g_s^r, & main - side\ lobe\ alignment \\ g_s^t g_m^r, & side - main\ lobe\ alignment \\ g_s^t g_s^r, & side - side\ lobe\ alignment \end{cases} \tag{3}$$

2.2. Beam-searching overhead

To overcome the deafness issue (misalignment between transmitter and receiver) in mmWave communication which is a direct consequence of using the directional antenna at both transmitter and receiver, beam-searching has been proposed. Beam-searching uses a sequence of pilot transmissions in an exhaustive fashion at both transmitter and receiver to establish the communication. It helps in finding the best beam between transmitter and receiver that provides the highest Signal to Interference plus Noise Ratio (SINR). However, finding the best beam is time-consuming and thus can affect the final throughput. For reducing the power consumption and beam-alignment overhead, our system model considers beam-searching technique proposed in [31]. The total searching (alignment) overhead for any link i under exhaustive beam-searching is given by:

$$\mathbb{T} = \left\lceil \frac{\psi_i^t}{\theta_i^t} \right\rceil \left\lceil \frac{\psi_i^r}{\theta_i^r} \right\rceil T_p \tag{4}$$

where, T_p is an average time required for a pilot transmission. $\mathbb{T}$ considers all combination of the directions of sector level beamwidth. ψ_i^t and ψ_i^r denote sector level beamwidths at transmitter and receiver, respectively, while θ_i^t and θ_i^r denote beam level beamwidths at the transmitter and receiver. In our study we consider equal beamwidth for the transmitter and receiver antennas i.e., $\theta_i^t = \theta_i^r = \theta$.

2.3. Channel model

Micro-urban Close-In (CI) path loss model proposed in [34] is considered in our system model. This model offers substantial simplicity and more stable behavior across different frequencies and distances. The path loss in CI model is calculated as follows:

$$PL(f,d) = K^{-1} d^n \tag{5}$$

$$K^{-1} = \left(\frac{4\pi f}{c}\right)^2 10^{(X_\sigma/10)} \tag{6}$$

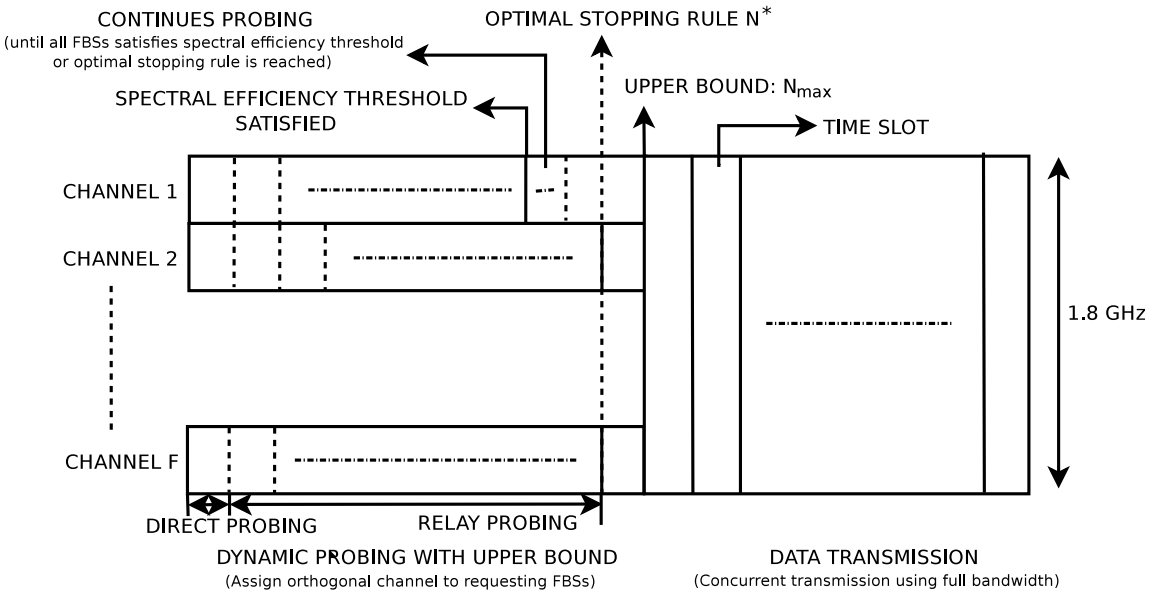

Fig. 3. Mode selection and data transmission.

where, $PL(f,d)$ denotes the path loss over frequency f at distance d from the transmitter, n denotes the single model parameter, c is the speed of light, and X_σ is the standard deviation describing large-scale signal fluctuations about the mean path loss over distance.

2.4. Independent and Identically Distributed (I.I.D.) Bernoulli blocking

Due to extremely high-frequency and smaller wavelength, mmWave signals are highly susceptible to obstacles like buildings, trees, hills, mountains, and, in some cases, high voltage electric power lines. These obstacles are spatially distributed in the radio environment and can cause high losses to mmWave links. To model these blocking events, we explicitly consider the random Bernoulli blockages in our system model. Across different links, blockages are assumed to be I.I.D. [29].

Let ρ denotes the probability that a link is blocked (or probability of occurrence of obstacles in between transmitter and receiver). We assume that a total average loss of b_{loss} (dB) occurs if a particular link is blocked. Let b_{ij} denote the average attenuation between the transmitter of link i and receiver of link j due to blocking event which is given by:

$$b_{ij} = (1-\rho) + \rho 10^{-b_{loss}/10} \tag{7}$$

We consider two different values of ρ given by p and p'. p is the probability that link between two FBSs is blocked, and p' is the probability that link between FBS and MiBS is blocked.

2.5. Mode selection and data transmission

In this section, we propose a mode selection, relaying, and concurrent data transmission protocol for mmWave based FBSs. According to our proposed protocol, the MiBS assigns orthogonal channels to requesting FBSs for mode and relay selection as shown in Fig. 3. Relays can provide an alternative multi-hop path for signals to reach the destination. However, determining whether a relay is appropriate or not needs learning of both source–relay (i.e., FBS-FBS (Relay)) and relay–destination (i.e., FBS (Relay)-MiBS) channels. For channel estimation, mmWave transmitter and receiver need to align their antenna beams towards each other and this beam alignment takes a non-negligible overhead. As stated earlier, probing more relays may increase the probability of finding a better relay but at the cost of more probing overhead. The overhead because of probing is calculated using Eq. (4).

Each FBS performs probing on its orthogonal channel in order to find its corresponding relay in case of relay mode of operation. The length of probing period can be different for different FBSs across various channels and frame period. Each frame period consists of two phases: probing (direct and relay) and data transmission phase. In probing phase, first probing slot is dedicated for direct probing in which FBSs directly probe to MiBS without using any relay. If the direct mode of communication is not possible then FBSs start searching for multihop path to MiBS by probing relays one-by-one. Probing is performed on independent channels in a distributed manner by FBSs while the link scheduling for data transmission is performed by MiBS using full bandwidth as shown in Fig. 3, which is the second phase of the protocol. The length of probing slot and data transmission slot is considered to be equal and is denoted as $\tau(=\mathbb{T})$. The total maximum duration of data transmission is T seconds. Let $|T|$ denote the number of data transmissions slots and the value of $|T|$ is given by $\lfloor T/\tau \rfloor$. Fig. 4 shows the complete sequence diagram of the proposed scheme. In our system model, MiBS controls the uplink and downlink transmissions of the FBSs in the network by suitably assigning the resources to the FBSs. MiBS broadcasts the beacons in all directions by activating its beams in all the sectors for synchronization and control information exchange. All the FBSs are assumed to have a backward compatibility and support 4G cellular communication. FBSs and the MiBS exchange data transmission requests, location information, and boresight direction using 4G cellular communication. Benefits of 4G+mmWave based network architecture are already shown in [25].

2.6. Mode selection for data transfer

The proposed system model uses two different modes of data transfer between an FBS and MiBS:

2.6.1. Direct mode of communication

In this mode an FBS transmits the data directly to the MiBS (mostly when there are no blockages/obstacles present between the FBS and MiBS link). Effective spectral efficiency achieved by FBS f at MiBS $m(=r_0)$ using direct mode of data transfer is given by:

$$S^f_{r_0} = log_2(1 + SNR_{f,m}) \tag{8}$$

where, $SNR_{f,m}$ represents Signal to Noise Ratio (SNR) of FBS-to-MiBS (F2M) link.

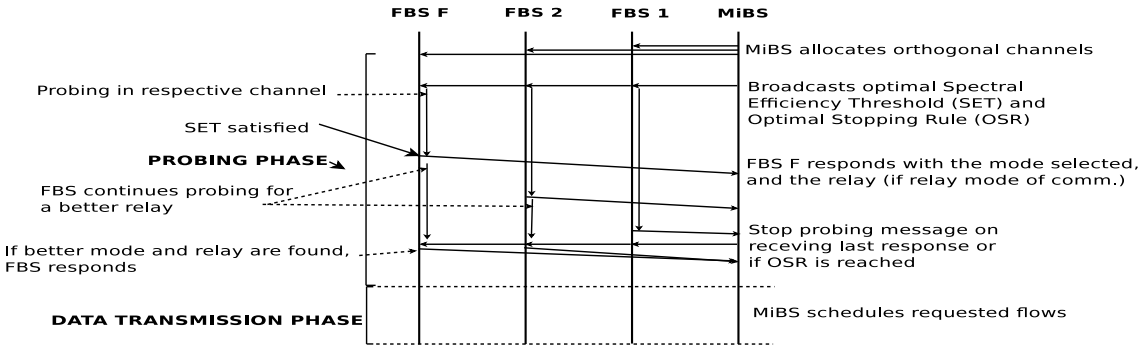

Fig. 4. Sequence diagram of proposed mode selection and data transmission scheme.

2.6.2. Relay mode of communication

In this mode the FBS uses other idle FBS as a relay for establishing communication to the MiBS. This mode of communication is used when direct mode of communication is not possible. Effective spectral efficiency achieved by FBS f using FBS r_i ($r_i \in Y$, $i \neq 0$) as a relay (using two hop decode and forward mechanism [35]) is given by:

$$S^f_{r_i} = \frac{1}{2} min\{log_2(1 + SNR_{f,r_i}), log_2(1 + SNR_{r_i,m})\} \tag{9}$$

where, SNR_{f,r_i} and $SNR_{r_i,m}$ represent the SNR of FBS-to-FBS (Relay) or F2F and F2M links, respectively. We assume time resources are equally divided between f, r_i and r_i, m transmissions when using relay mode of data transmission. We consider zero processing delay at the relay FBS r_i.

2.7. SINR and Bitrate

Let the distance between the transmitter t_i of link i and the receiver r_j of link j is given by $d_{ij} (= d_{ji})$. Let g^t_{ij} and g^r_{ji} denote the antenna gain of t_i in the direction of r_j, and the antenna gain of r_j in the direction of t_i, respectively. Considering path loss over the distance and gains due to antennas, the received signal power at r_i from t_i is given by:

$$P_r(i,i) = K P_t g^t_{ii} g^r_{ii} d^{-n}_{ii} b_{ii} \tag{10}$$

Similarly, the received interference at r_i from t_j ($j \neq i$) under concurrent transmissions is given by:

$$P_r(j,i) = K P_t g^t_{ji} g^r_{ij} d^{-n}_{ji} b_{ji} \tag{11}$$

where, $g^t_{ii} g^r_{ii}$ and $g^t_{ji} g^r_{ij}$ take one of the values given in Eq. (3), depending upon lobe alignment. The SINR Γ_j of an FBS in the F2F link j and the SINR Γ_c of the MiBS in F2M link c during uplink transmission are given by:

$$\Gamma_j = \frac{P_r(j,j)}{\sum_{i \in \mathcal{A},\ i \neq j} P_r(i,j) x^\tau_i + \sum_{i \in \mathcal{B}} P_r(i,j) x^\tau_i + \sigma^2 W} \tag{12}$$

$$\text{and} \quad \Gamma_c = \frac{P_r(c,c)}{\sum_{i \in \mathcal{A}} P_r(i,c) x^\tau_i + \sum_{i \in \mathcal{B},\ i \neq c} P_r(i,c) x^\tau_i + \sigma^2 W}, \tag{13}$$

respectively. Here, $\mathcal{A}$ and $\mathcal{B}$ represent the set of F2F and F2M links, respectively. P_t is the maximum transmit power of the FBS. W is the channel bandwidth. σ^2 is the Additive White Gaussian Noise. x^τ_i is a indicator variable defined as:

$$x^\tau_i = \begin{cases} 1 & \text{if link } i \in \{\mathcal{A} \cup \mathcal{B}\} \text{ is scheduled} \\ & \text{in data slot } \tau \\ 0 & \text{otherwise} \end{cases} \tag{14}$$

Using Shannon's capacity theorem [36], the expected achievable data rates R_j and R_c of F2F and F2M, respectively can be given by:

$$R_j = W log_2(1 + \Gamma_j) \text{ and} \tag{15}$$

$$R_c = W log_2(1 + \Gamma_c), \tag{16}$$

3. Problem formulation

3.1. Problem formulation

Our problem objective consists of two independent folds —

3.1.1. Determining the best stopping rule criteria for probing

Probing more relays when the direct mode of communication is not possible may increase the probability of finding a better relay but at the cost of more probing overhead. The increase in probing overhead will affect the flow throughput, which in turn influences the system throughput. Hence, the objective of this problem is to determine the best stopping rule $N^* \in [0, n']$ for probing which performs a finite number of probes and maximizes the flow throughput $\mathcal{R}^f$. N^* also includes the first probe overhead because of direct mode of communication.

An optimization formulation for this problem is given as:

$$maximize\{\mathcal{R}^f\} \ \forall \ f \in F \tag{17}$$

where, $\mathcal{R}^f$ is given by:

$$\mathcal{R}^f = W \left(\frac{T}{T + T_f} \right) max\{S^f_{r_i}\},\ 0 \leq i \leq n' \tag{18}$$

When probing a relay r_i, whether relay–destination link $r_i - m$ is probed or not depends upon the probing output of source–relay link $f - r_i$. Indicator variable Λ_{f,r^f_i} accounts for the same. Thus, probing overhead T_f represents the total time duration for probing by FBS f, and is given by:

$$T_f = \sum_{i=0}^{n'} (\tau + \tau \Lambda_{f,r^f_i}) \tag{19}$$

where, Λ_{f,r^f_i} is calculated as:

$$\Lambda_{f,r^f_i} = \begin{cases} 1 & if\ 0.5 log_2(1 + SNR_{f,r^f_i}) \geq \gamma, \text{ where } i \neq 0 \\ 0 & i = 0 \text{ and } otherwise \end{cases} \tag{20}$$

subject to,

$$n' \leq |Y| \tag{21}$$

where, $|Y|$ is the number of idle relays present in the network. In Eq. (19), first term τ under summation is probing overhead because of the source–relay probe, and the second term $\tau \Lambda_{f,r^f_i}$ is probing overhead because of the relay–destination probe. γ is the spectral efficiency threshold. Note that indicator variable Λ_{f,r^f_i} is equals to zero when $i = 0$ because it is the case for direct mode of communication and no relay is involved in first probe. FBSs are given the orthogonal channels for probing. In order to maximize the average flow throughput (single hop or multi-hop) as described above, it is important to find the optimal stopping rule N^*.

3.1.2. Maximization of number of concurrent transmissions

The objective of this part of the problem is to maximize the number of concurrent flow transmissions. The flow requests have been modeled as a graph $G = (V, E)$, where $V = \{D \cup R\}$ is the set of Direct and Relay (two-hop) requests received by MiBS for data transmission in a particular frame and E is the set of edges between the flow request V. If $(i, j) \in E$ then the transmissions due to flows i and j interfere with each other and cannot be scheduled together. x_i^τ is defined as:

$$x_i^\tau = \begin{cases} 1 & if\ flow\ i\ is\ scheduled\ on\ data\ slot\ \tau \\ 0 & otherwise \end{cases} \tag{22}$$

In order to maximize the number of flows scheduled in our system, we maximize the utilization of the data slots of a frame, which can be represented as follows:

$$\max \sum_{\tau \in T} \sum_{i \in V} x_i^\tau \tag{23}$$

such that,

$$x_i^\tau + x_j^\tau \leq 1 \quad \text{where, } (i, j) \in E,\ \forall i, \forall j; j \neq i, \forall \tau \tag{24}$$

where, $|T|$ is the number of data transmission slots available in one frame. Constraint (24) ensures that the two interfering flows i and j cannot be scheduled concurrently in the same data slot τ. The optimization problem can be mapped to finding a maximal independent set problem which is a well-known NP-hard problem. The search space is $2^{|D|+|R|}$ if MiBS uses exhaustive searching for scheduling the backhaul flows. In order to solve the problem, we propose a polynomial-time heuristic scheduling algorithm in the next section.

In this paper, we consider the location of FBSs to be fixed. It is important to note here that irrespective of this assumption the problem of beam searching/training, searching for good relays, and the scheduling cannot be solved as an offline problem and needs good heuristics to solve. This is because the mmWave band is highly susceptible to the blockages, hence, even if the transmitters and receivers are fixed, backhaul link budget can be significantly affected by the moving/dynamic blockages coming in between the transmitters and receivers. This creates the need for dynamic relay probing and scheduling decisions.

4. Proposed solution

As stated in Section 2.5, MiBS allocates orthogonal channel to each of the FBSs on receiving the data transfer requests for probing. Each FBS performs probing on its corresponding allocated channel, in a distributed manner. On every channel, first, FBS-MiBS link is probed using direct mode of data transmission. An FBS performs the direct probing in the first data slot of the allocated channel in every frame interval. If the direct mode provides the required spectral efficiency threshold γ, then the FBS sends feedback to MiBS stating direct mode satisfies γ and continues probing in order to find a better relay. However, if there is no more probing allowed (N^* is reached) then FBS stops probing, and the direct mode of transmission is selected. Next, the FBS requests MiBS for scheduling the flow to transmit the data.

On the other hand, if the direct mode of transmission does not provide the required spectral efficiency, FBS starts relay probing for finding an alternate multihop path to MiBS. In relay probing, if first FBS-FBS (Relay) is blocked, probing stops for that relay; otherwise, the FBS(Relay)-MiBS link is further probed. Each FBS performs probing on its allocated channel until the spectral efficiency threshold is satisfied or N^* is reached. If the spectral efficiency threshold is achieved, each FBS feedbacks the FBS (Relay) for which flow throughput is maximum. It is also important to note that probing can also be stopped once the response from all the FBSs is received. MiBS sends stop probing message to all the FBSs in order to perform this action as shown in Fig. 4. On receiving stop probing message from MiBS, all the FBSs will convey their best mode and the best relay (in case of relay mode is better than the direct mode) to the MiBS. Once the probing phase completes MiBS schedules all the flows in data transmission phase.

The number of probes or number of time slots required by each FBS can be different, however, are bounded by N_{max} to prevent unnecessary overhead because of probing in our protocol design as shown in Fig. 3. Here, N_{max} denotes the maximum number of probes. We are interested in determining the optimal value of number of probes N^* (which is less than equals to N_{max}) which maximizes the flows throughput.

In order to determine the value of N^*, we define two propositions based on single FBS and multiple FBSs scenarios, such that flows throughput is maximized.

Proposition 1. *The optimal number of relays to be probed in single FBS scenario is given by:*

$$p^* = \min\{n \in [0, |Y|]; S_{r_n}^f \geq \frac{s^*}{W}\} \tag{25}$$

where, s^* is the maximum throughput achieved by the FBS f, if it is allowed to probe 0 to $|Y|$ relays. The value of s^* can be obtained by varying the spectral efficiency threshold γ. According to the proof in [29], probing can be certainly stopped once spectral efficiency threshold s^*/W is achieved, and at that point, average throughput will be maximum. The proof does not consider the direct mode of communication, however, it is still applicable by changing the domain of n from natural numbers to whole numbers. Hence, the optimal number of probes N^* (optimal stopping rule criteria) for the single FBS scenario corresponding to p^* is given by:

$$N^* = \sum_{i=0}^{p^*} (1 + \Lambda_{f, r_i^f}) \tag{26}$$

Proposition 2. *MiBS uses the following heuristic for determining stopping rule criteria for multiple FBS scenario, which is given by:*

$$N_m^* = \min\{N^*, \max_{f \in F}\{N_f\}\} \tag{27}$$

Here, N_f represents the number of probes required by FBS f in order to satisfy the optimal spectral threshold s^*/W as discussed in Proposition 1. The stopping rule criteria for multiple FBSs scenario is either N^* (if $\min\{N^*, \max_{f \in F}\{N_f\}\}$ is equal to N^*), or it corresponds to FBS f with maximum N_f. The values of N^* and N_m^* are bounded by N_{max}.

It is important to note that each FBS may end up with a different number of probes. Thus, we limit the number of probes with an upper bound N^*. Here, N^* is the optimal stopping rule criteria for single FBS scenario. As relay probing is performed and repeated independently across different frame period and across different channels by FBSs, the number of relays that are probed can be different, and thus the value of $max_{f \in F}\{N_f\}$ may be different at a different frame period. Algorithm 1 presents the distributed mode selection and relay selection pseudo code. Computational complexity of Algorithm 1 is $O(N^*)$. After probing phase, MiBS starts concurrently scheduling all the single and two-hop flows by using the interference constraints defined in the next section.

4.1. Analyzing Single Transmission (TDMA) vs. concurrent transmissions by considering blockages

In the case of TDMA, link transmissions happen in rapid succession, one after the other, each using its own time slot. Hence, the link does not suffer interference from any other ongoing transmissions. Let j and c denote the F2F and F2M links, respectively, then the average data rates R_j' and R_c' that can be achieved by links j and c, respectively, using TDMA are given by:

$$R_j' = \frac{W}{|T|} \log_2 \left(1 + \frac{P_r(j, j)}{\sigma^2 W}\right) \tag{28}$$

$$R_c' = \frac{W}{|T|} \log_2 \left(1 + \frac{P_r(c, c)}{\sigma^2 W}\right) \tag{29}$$

Algorithm 1 Distributed Mode and Relay Selection Algorithm

```
procedure DMRS
    n' ← 0
    for n = 0 to N* do
        if S^f_{r_n} ≥ s*/W then
            if n equals 0 then
                direct mode selected by FBS f
                send feedback to MiBS
            else
                relay mode selected by FBS f
                n' ← arg max{R^f_{r_n}}
                r_{n'} is selected as relay
                feedback mode & relay information to MiBS
            end if
        else
            probe next idle relay
        end if
    end for
    request MiBS for scheduling
end procedure
```

In the case of concurrent transmissions, multiple links can be scheduled concurrently. Thus, the links may suffer interference from other links. In that case, the average data rates R_j and R_c, achieved by links j and c, respectively, are derived in Eqs. (15) and (16).

To achieve $R_j \geq R'_j$ and $R_c \geq R'_c$, we have derived a sufficient condition in our previous work [6]. The condition ensures that average data rate achieved by each link in case of concurrent transmission can be higher than that of TDMA if we allow links whose mutual interference is less than the background noise. In the previous work, the constraints derived from the sufficient condition do not explicitly consider the effect of blockages. However, using the same sufficient condition, we have derived the interference distance constraints by explicitly considering blockages in the next subsection.

4.2. Interference distance constraints

Different kinds of interference possible among flows in case of uplink scenario are as follows:

1. A direct flow interfering with another direct flow.
2. A relay flow interfering with another relay flow.
3. A relay flow interfering with other direct flow and vice-versa

As FBSs and MiBS are employed with the directional antennas in our system model, the interference power mostly depends on the alignment of lobes. For a fixed distance in general, the interference will be maximum when the interfering transmitter and receiver main lobes are aligned when there are no blockages. On the other hand, it will be minimum when side lobes are aligned. For achieving the better system throughput non-interfering flows should be scheduled concurrently. As discussed in the previous section, for scheduling two links concurrently, interference experienced at the receiver of link i (j) from the transmitter of link j (i) should be less than or equal to the background noise. In this work, we assume a single blockage of average loss $10^{\frac{b_{loss}}{10}}$ which is the aggregate average loss because of all the obstacles present between transmitter and receiver. Based on the four different possibilities of transmitter and receiver lobe alignments, we derive four different interference distance thresholds considering corresponding total gain at transmitter and receiver.

4.2.1. Constraint 1: Main lobe-main lobe alignment

Transmitter Tx_i and interfered receiver Rx_j are said to be main lobes aligned with each other when interfering transmitter is in beamwidth of interfered receiver ($\Delta_i \leq \theta/2$), and the interfered receiver is in beamwidth of interfering transmitter ($\Delta_j \leq \theta/2$). However, Tx_i will interfere with Rx_j only when the $d \leq d_{mm}$, where d is the distance between Tx_i and Rx_j. Geometry to determine Δ_i and Δ_j is shown in Fig. 5. d_{mm} represents the maximum interference range of Tx_i (when main lobe of Tx_i is aligned with main lobe of Rx_j) which is given as:

$$d_{mm} = \left(\frac{K g_m^t g_m^r P_t((1-p) + p10^{-b_{loss}/10})}{\sigma^2 W} \right)^{1/n} \tag{30}$$

As shown in Fig. 6, interfering transmitter T and receiver $R2$ are main lobe-main lobe aligned and the distance between them is less than d_{mm}, thus T will interfere with $R2$. For data transfer, it is the most desirable alignment and we assume that the main lobes of the transmitter and receiver of a link i are aligned before data transfer in order to maximize the data transfer rate and to avoid the deafness problem.

4.2.2. Constraint 2: Main lobe-side lobe alignment

Main lobe of interfering transmitter Tx_i and side lobe of interfered receiver Rx_j are aligned with each other if $\Delta_i \leq \theta/2$ and $\Delta_j \geq \theta/2$. It is the case when Rx_j is within the beamwidth of Tx_i and Tx_i is outside the beamwidth of Rx_j. However, if $d \geq d_{ms}$, Rx_j will not get interfered by Tx_i. Here, d_{ms} represents the maximum interference range of Tx_i (when main lobe of Tx_i is aligned with side lobe of Rx_j) which is given as:

$$d_{ms} = \left(\frac{K g_m^t g_s^r P_t((1-p) + p10^{-b_{loss}/10})}{\sigma^2 W} \right)^{1/n} \tag{31}$$

In Fig. 6, transmitter T and receiver $R4$ are main lobe-side lobe aligned, and $R4$ is in interfering range of T as the distance between them is less than d_{ms}.

4.2.3. Constraint 3: Side lobe-main lobe alignment

Side lobe of interfering transmitter Tx_i and main lobe of interfered receiver Rx_j are aligned with each other if $\Delta_i \geq \theta/2$ and $\Delta_j \leq \theta/2$. It is the case when Rx_j is outside the beamwidth of Tx_i and Tx_i is within the beamwidth of Rx_j. However, Rx_j will not get interfered by Tx_i, if $d \geq d_{sm}$, where d_{sm} is given as:

$$d_{sm} = \left(\frac{K g_s^t g_m^r P_t((1-p) + p10^{-b_{loss}/10})}{\sigma^2 W} \right)^{1/n} \tag{32}$$

In Fig. 6, transmitter T and receiver $R6$ are side lobe-main lobe aligned, and $R6$ is in interfering range of T as distance between them is less than d_{sm}.

4.2.4. Constraint 4: Side lobe-side lobe alignment

If $\Delta_i \geq \theta/2$ and $\Delta_j \geq \theta/2$ then the side lobe of interfering transmitter Tx_i and the side lobe of interfered receiver Rx_j is aligned. It is the case when Rx_j is outside the beamwidth of Tx_i, and vice-versa. However, Rx_j will not get interfered by Tx_i if $d \geq d_{ss}$, where d_{ss} is given as:

$$d_{ss} = \left(\frac{K g_s^t g_s^r P_t((1-p) + p10^{-b_{loss}/10})}{\sigma^2 W} \right)^{1/n} \tag{33}$$

In Fig. 6, transmitter T and receiver $R5$ are side lobe-side lobe aligned, and $R5$ is in interfering range of T as distance between them is less than d_{ss}.

4.3. Interference matrix

MiBS and FBSs use the maximum transmission power to compute the interfering distance as described above. MiBS uses Constraint 1 to Constraint 4 for determining whether two F2F links or F2M and F2F links are non-interfering. However, for checking two F2M links to be non-interfering for uplink transmission MiBS uses the condition $|\phi_1 - \phi_2| > \theta'$ as shown in Fig. 7. It is so because we have assumed zero gain because of the side lobe of MiBS. This constraint allows the

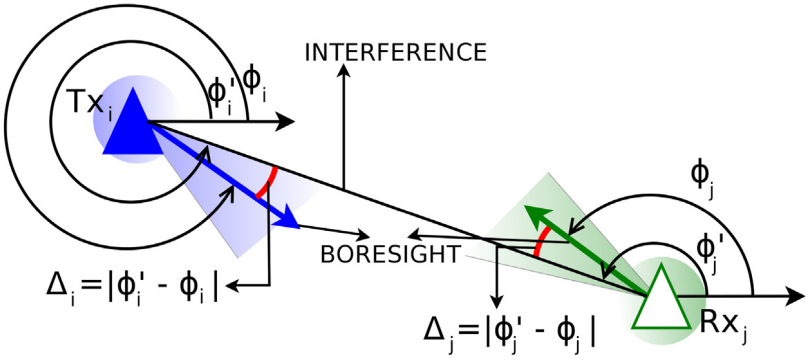

Fig. 5. Lobe alignment.

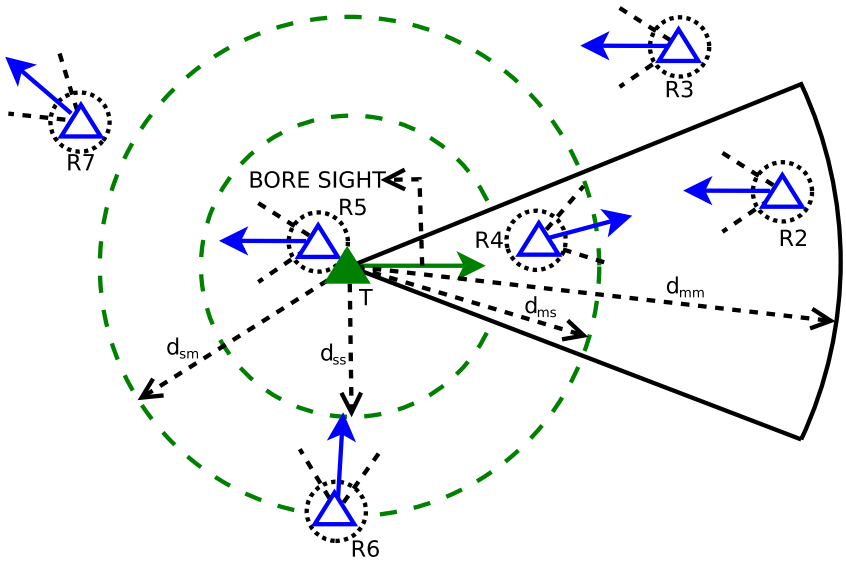

Fig. 6. Interference region.

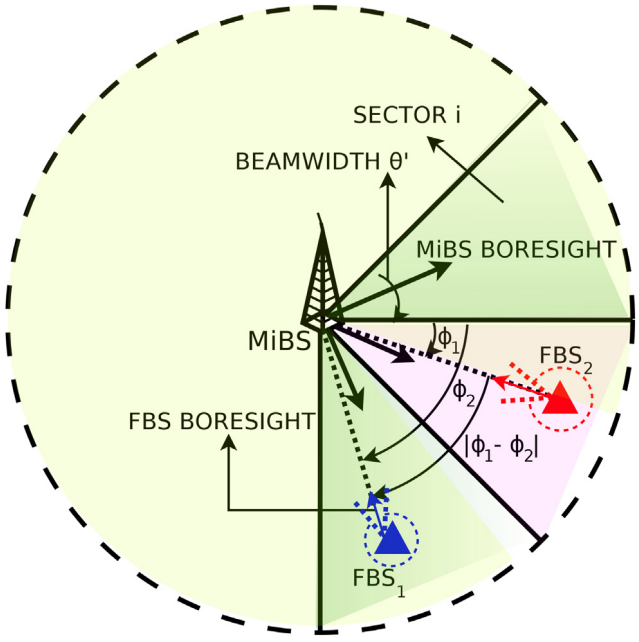

Fig. 7. Concurrent uplink transmission from two FBSs.

maximum of one F2M transmission in a sector. All the derived interfering range constraints well account for blockages and their probability of occurrence is terrain dependent.

For scenario 1, i.e., two direct flows are considered to be non-interfering if they belong to the different sectors. i.e, they should satisfy the constraint $|\phi_1 - \phi_2| > \theta'$. On the other hand for scenario 2, two relay flows $f1 - r1 - m$ and $f2 - r2 - m$ are said to be non-interfering if their corresponding F2Fs links ($f1 - r1$ and $f2 - r2$) and F2M links ($r1 - m$ and $r2 - m$) are non-interfering. It is important to note that as we consider half duplex transceiver design the condition for scenario 2 will work exactly fine. For scenario 3, a direct flow ($f1 - m$) and a relay flow ($f2 - r2 - m$) are considered to be non-interfering if links $f1 - m$ and $f2 - r2$, and links $f1 - m$ and $r2 - m$ are non-interfering. $f1 - m$ is given the full data slot. However, $f1 - r2$ is scheduled in first half data slot and on the other hand $r2 - m$ is scheduled in the next half data slot because of half duplex transceiver design assumption.

All the interference related information is stored in a concise interference matrix at MiBS. The interference matrix acts as a look-up table for the scheduling decision and helps in taking efficient scheduling decisions. MiBS updates the interference matrix based on the new active flow requests. Interference matrix contains binary entries (1 or 0) and is updated based on the interference distance constraints derived in Section 4.2. MiBS uses interference matrix of size $|V| \times |V|$, where $|V|$ is the total number of requests including both direct and relay flows. In the proposed interference matrix, let $IM(i, j)$ (element at ith row and jth column) represent the interference between the flows i and j. If i and j cannot be scheduled together due to high interference then

the value $IM(i,j)$ will be 1, 0 otherwise. MiBS uses Algorithm 2 for computing the interference matrix.

Algorithm 2 Interference Matrix Determination

```
1: procedure findInterferenceMatrix(V)
2:     for each i ∈ V do
3:         for each j ∈ V − i do
4:             d ← getDistance(Tx_i, Rx_j)
5:             if (i ∈ R & j ∈ R) or (i ∈ D & j ∈ R) or (i ∈ R & j ∈ D) then
6:                 if (∠Δ_i ≤ θ/2 & ∠Δ_j ≤ θ/2 & d ≤ d_mm) or (|φ_1 − φ_2| ≤ θ′) then
7:                     IM(i, j) ← 1
8:                 else if (∠Δ_i ≤ θ/2 & ∠Δ_j ≥ θ/2 & d ≤ d_ms) or (|φ_1 − φ_2| ≤ θ′)
   then
9:                     IM(i, j) ← 1
10:                else if (∠Δ_i ≥ θ/2 & ∠Δ_j ≤ θ/2 & d ≤ d_sm) or (|φ_1 − φ_2| ≤ θ′)
   then
11:                    IM(i, j) ← 1
12:                else if (∠Δ_i ≥ θ/2 & ∠Δ_j ≥ θ/2 & d ≤ d_ss) or (|φ_1 − φ_2| ≤ θ′)
   then
13:                    IM(i, j) ← 1
14:                else
15:                    IM(i, j) ← 0
16:                end if
17:            else if (i ∈ D & j ∈ D) then
18:                if |φ_1 − φ_2| > θ′ then
19:                    IM(i, j) ← 0
20:                else
21:                    IM(i, j) ← 1
22:                end if
23:            end if
24:        end for
25:    end for
26: end procedure
```

4.4. Concurrent Flow Scheduling (CFS)

In this section, we propose an efficient polynomial time scheduling algorithm using interference matrix defined in the previous section. As shown in Section 3, flow scheduling is a complex problem, thus, we use various heuristics proposed in Section 4.2 for taking scheduling decisions. The mobility of FBSs is ignored while taking the scheduling decision as the position of FBSs is assumed to be fixed at the rooftop (as stated in Section 2). Hence, the received signal power and interference power at the receiving base station will not change significantly. We have assumed that MiBS has a global knowledge of the network topology e.g., location of the FBSs, number of active flows etc.

MiBS uses full bandwidth for concurrently scheduling all the single and multihop requests as shown in Fig. 3. MiBS maintains two different queues $DReqQ$ and $RReqQ$ for direct and relay mode requests, respectively. SQ_i contains all the flows that can be scheduled concurrently in slot i without interfering with each other. Algorithm 3 (CFS) describes the procedure of scheduling the backhaul flows. MiBS executes CFS algorithm at regular intervals of time. CFS loops until all the direct and relay mode requests are scheduled.

In order to achieve fairness among direct flow requests and among relay flow requests, we maintain a separate counter C_f for all the flows. Counter C_f for a flow is incremented by one, once it successfully gets the slot to schedule. Functions $extractDirectReq()$ and $extractRelayReq()$ help in achieving the fairness. These functions sort the respective flows direct and relay in non-descending order based on their C_f value, and randomize the flows with same C_f values. Sorting of flows might increase the computational complexity, but it is necessary to achieve the fairness among flows. On the other hand, in order to achieve fairness among the queues, MiBS gives priority to $DReqQ$ and $RReqQ$ alternatively, i.e., in even numbered slots first, $DReqQ$ are checked for scheduling followed by $RReqQ$. However, in odd numbered slots it is in reverse order (i.e., $RReqQ$ are checked for scheduling followed by $DReqQ$). In the even numbered slots (line 8–10), MiBS first tries to schedule all the non-interfering direct flow requests (line 9). And, all the interfering direct flow requests are added to $DReqNQ$ for the candidate to be scheduled in next data slot (line 15). Once all the direct requests present in $DReqQ$ are polled, MiBS starts adding non-interfering relay mode requests to the SQ_i (line 10). Similarly, in the odd numbered slots (line 11–13), MiBS first tries to schedule all the non-interfering relay flows requests (line 12). Here, all the interfering relay flow requests are added to $RReqNQ$ for the candidate to be scheduled in the next slot (line 16). Once all the relay requests present in $RReqQ$ are polled, MiBS starts adding non-interfering direct mode requests to the SQ_i (line 13). Algorithms 4 and 5 are the procedures for adding non-interfering direct and relay flows in a slot SQ_i, respectively. For determining whether two flows are interfering MiBS uses interference matrix. Time complexity of Algorithm 3 to allocate time slot is $O((D+R)^2 + Dlog(D) + Rlog(R))$. $O(Dlog(D))$ and $O(Rlog(R))$ are the time complexities to sort direct flow requests and relay flow requests, respectively. $O((D+R)^2)$ is the computational complexity of comparisons between flows for scheduling non-interfering flows only.

Algorithm 3 Concurrent Flow Scheduling

```
1: procedure CFS(V)
2:     i ← 0
3:     IM ← findInterferenceMatrix(V)
4:     DReqQ ← extractDirectReq(V)
5:     RReqQ ← extractRelayReq(V)
6:     while DReqQ is not empty or RReqQ is not empty do
7:         SQ_i ← null
8:         if (i modulo 2 == 0) then
9:             (DReqNQ,SQ_i) ← DSDL(DReqQ, IM, SQ_i)
10:            (RReqNQ,SQ_i) ← RSDL(RReqQ, IM, SQ_i)
11:        else
12:            (RReqNQ,SQ_i) ← RSDL(RReqQ, IM, SQ_i)
13:            (DReqNQ,SQ_i) ← DSDL(DReqQ, IM, SQ_i)
14:        end if
15:        DReqQ ← DReqNQ
16:        RReqQ ← RReqNQ
17:        i ← i + 1
18:    end while
19: end procedure
```

Algorithm 4 Direct Flows Scheduling

```
1: procedure DSDL(DReqQ, IM, SQ_i)
2:     if SQ_i is empty and DReqQ is not empty then
3:         SQ_i.add(DReqQ.remove())
4:     end if
5:     while DReqQ is not empty do
6:         for all flow_i ∈ DReqQ do
7:             for all flow_j ∈ SQ_i do
8:                 if IM[flow_i][flow_j] = 0 then
9:                     SQ_i.add(DReqQ.remove())
10:                else
11:                    DReqNQ.add(DReqQ.remove())
12:                end if
13:            end for
14:        end for
15:    end while
16:    return (DReqNQ, SQ_i)
17: end procedure
```

In our proposed scheme, scheduling is performed in the scheduling phase of every frame. Also, when a new flow is added or dropped. It is important to note that MiBS gives the complete data slot to direct flows. However, for relay flows, half slot is allocated to FBS-FBS (Relay), followed by rest of the half data slot to FBS (Relay)-MiBS for

Algorithm 5 Relay Flows Scheduling

```
procedure RSDL(RReqQ, IM, SQ_i)
    if SQ_i is empty and RReqQ is not empty then
        SQ_i.add(RReqQ.remove())
    end if
    while RReqQ is not empty do
        for all flow_i ∈ RReqQ do
            for all flow_j ∈ SQ_i do
                if IM[flow_i][flow_j] = 0 then
                    SQ_i.add(RReqQ.remove())
                else
                    RReqNQ.add(RReqQ.remove())
                end if
            end for
        end for
    end while
    return (RReqNQ, SQ_i)
end procedure
```

scheduling. As we consider half duplex transceiver design, FBSs cannot perform transmission and reception at the same time.

5. Analysis

In this section, we propose a probabilistic analysis to mathematically evaluate the expected number of concurrent transmissions possible with different antenna configurations and the number of direct and relay flows requests, for our proposed scheduling algorithm. Consider a circular region of radius R_ψ, with m direct and n relay based active flows requesting for data transfer. We define $P(a,b,m,n)$ as the probability that a out of m direct flows and, b out of n relay based flows can be scheduled concurrently in the same slot, and is given by:

$$P(a,b,m,n) = \widetilde{\mathcal{P}}(a,m)\mathcal{P}'((b,n)|(a,m)) \tag{34}$$

where, $\mathcal{P}'((b,n)|(a,m))$ is the probability that b out of n relay flows can be scheduled concurrently given that a out of m direct flows can be scheduled in the same slot and are present in set SQ_i. $\widetilde{\mathcal{P}}(a,m)$ is the probability that a out of m direct flows can be scheduled concurrently and are added to the set SQ_i. Here, SQ_i contains all the non-interfering flows that can be scheduled concurrently in the ith slot.

We define P_{mm}, P_{ms}, P_{sm}, and P_{ss} as the probabilities of Main lobe-Main lobe, Main lobe-Side lobe, Side lobe-Main lobe, and Side lobe-Side lobe alignment, respectively. P_{mm}, P_{ms}, P_{sm}, and P_{ss} are given by:

$$P_{mm} = \left(\frac{\theta}{2\pi}\right)^2,\ P_{ms} = \left(\frac{\theta}{2\pi}\right)\left(1-\frac{\theta}{2\pi}\right),$$
$$P_{sm} = \left(1-\frac{\theta}{2\pi}\right)\left(\frac{\theta}{2\pi}\right),\ \text{and}\ P_{ss} = \left(1-\frac{\theta}{2\pi}\right)^2 \tag{35}$$

Each flow (direct or relay) has certain probability with which it can be concurrently scheduled with the other flows (direct or relay). According to heuristic defined in Section 4.2, for scheduling two direct flows they should belong to different sectors. Thus, the probability $P^{\widetilde{D}}_{\widetilde{D}}$ of scheduling two direct flows concurrently is given by:

$$P^{\widetilde{D}}_{\widetilde{D}} = 1 - \left(\frac{\theta}{2\pi}\right) \tag{36}$$

Two relay flows $f1-r1-m$ and $f2-r2-m$ are said to be non-interfering if $f1-r1$ and $f2-r2$, and $r1-m$ and $r2-m$ are non-interfering as we consider half duplex transceiver design. $f1-r1$ and $f2-r2$ are said to be non-interfering if $r1$ and $r2$ are lying outside the interfering range of $f2$ and $f1$, respectively, and its probability is given by $(1-(P_{mm}Q_{mm}+P_{ms}Q_{ms}+P_{sm}Q_{sm}+P_{ss}Q_{ss}))^2$. However, for $r1-m$ and $r2-m$ to be non-interfering they should belong to different sectors, and its probability is given by $(1-\frac{\theta}{2\pi})$. Thus, the probability $P^{\widetilde{R}}_{\widetilde{R}}$ of scheduling two relay flows concurrently is given by:

$$P^{\widetilde{R}}_{\widetilde{R}} = (1-(P_{mm}Q_{mm}+P_{ms}Q_{ms}+P_{sm}Q_{sm} + P_{ss}Q_{ss}))^2\left(1-\frac{\theta}{2\pi}\right) \tag{37}$$

where, Q_{mm}, Q_{ms}, Q_{sm}, and Q_{ss} are the probabilities of the interfered receiver being present in a particular region. Here Q_{ij} is given by $Q_{ij} = A_{ij}/(\pi R_\psi^2)$ where $i,j \in \{s,m\}$. Fig. 6 shows the four different interference regions based on different lobe alignments and A_{ij} represents the area of that corresponding region.

A direct flow $f1-m$ and a relay flow $f2-r2-m$ are said to be non-interfering, if $f2$ is outside the sector of $f1-m$ transmission (as gain due to side lobe of MiBS is considered to be zero), and its probability is given by $(1-\frac{\theta}{2\pi})$, and $r2$ is outside the interfering region of $f1$, probability of which is given by $(1-(P_{mm}Q_{mm}+P_{sm}*Q_{sm}))$ ($Q_{sm}=Q_{ss}=0$ as gain of side lobe is considered to be zero). Also, $f1-m$ and $r2-m$ should be non-interfering whose probability is given by $(1-\frac{\theta}{2\pi})$. Thus, the probability $P^{\widetilde{R}}_{\widetilde{D}}$ of scheduling a direct flow and a relay flow concurrently is given by

$$P^{\widetilde{R}}_{\widetilde{D}} = \left(1-\frac{\theta}{2\pi}\right)(1-(P_{mm}Q_{mm}+P_{sm}*Q_{sm}))\left(1-\frac{\theta}{2\pi}\right) \tag{38}$$

In [19], authors have derived the probability expression/recursive definition for finding the probability of concurrent transmissions for single type of link scenario. However, in this analysis, we extend it to the case when two different types of flows can exist in the system, with different probabilities of scheduling with each other.

After checking m direct flows, and before checking relay flows, there can be a direct flows in set SQ_i, if (i) there are $a-1$ direct flows in set SQ_i when we check the first $m-1$ direct flows, and mth direct flow does not conflict with the other $m-1$ direct flows in SQ_i, or (ii) there are a direct flows in the set when we check the first $m-1$ direct flows, and the mth direct flow conflicts with any of the other $a-1$ flows in SQ_i. Thus, $\widetilde{\mathcal{P}}(a,m)$ is given by:

$$\widetilde{\mathcal{P}}(a,m) = \widetilde{\mathcal{P}}(a-1,m-1)(P^{\widetilde{D}}_{\widetilde{D}})^{a-1} + \widetilde{\mathcal{P}}(a,m-1)(1-(P^{\widetilde{D}}_{\widetilde{D}})^a)\ for\ a<m \tag{39}$$

We define boundary cases for the above recurrence as follows:

Case 1: After checking m direct flows, and before checking relay flows, only first direct flow can be in the set SQ_i. It implies that next $m-1$ direct flows are interfering, and cannot be scheduled concurrently. Thus, the probability of this case is given by:

$$\widetilde{\mathcal{P}}(1,m) = (1-P^{\widetilde{D}}_{\widetilde{D}})^{m-1}\ for\ a=1 \tag{40}$$

Case 2: Another boundary case can be m direct flows scheduled concurrently in the same slot implying that none of the direct flows conflict with the other direct flows.

$$\widetilde{\mathcal{P}}(m,m) = (P^{\widetilde{D}}_{\widetilde{D}})^{m_{C_2}}\ for\ a=m \tag{41}$$

After checking m direct flows followed by n relay flows there can be a direct and b relay flows in the set SQ_i, if (i) a out of m direct flows are non-interfering with any other flow present in the set SQ_i, and (ii) b out of n relay flows are non-interfering with any other flows present in the set SQ_i.

Set SQ_i contains a direct flows followed by b relay flows, if (i) there are a direct flows in set SQ_i when we check the first $n-1$ relay flows and nth relay flow does not conflict with the other a direct flows and $b-1$ relay flows in the set SQ_i, (ii) there are a direct flows followed by b relay flows when we check first $n-1$ relay flows and nth relay flow conflict with one of the flows (direct or relay) in the set SQ_i. Thus, the probability $\mathcal{P}'((b,n)|(a,m))$ of scheduling b out of n relay flows concurrently given that a out of m direct flows can schedule in the same slot, is given by:

$$\mathcal{P}'((b,n)|(a,m)) = \mathcal{P}'((b-1,n-1)|(a,m))(P^{\widetilde{R}}_{\widetilde{D}})^a(P^{\widetilde{R}}_{\widetilde{R}})^{b-1} + \mathcal{P}'((b,n-1)|(a,m))(1-(P^{\widetilde{R}}_{\widetilde{D}})^a(P^{\widetilde{R}}_{\widetilde{R}})^b) \tag{42}$$

Case 3: All the n relay flows can be scheduled concurrently with a direct flows and its probability is given by

$$\mathcal{P}'((n,n)|(a,m)) = (P_{\widetilde{D}}^{\widetilde{R}})^{an}(P_{\widetilde{R}}^{\widetilde{R}})^{nC_2} \quad for\ b = n \tag{43}$$

Case 4: Another possibility can be that a direct flows can be added to SQ_i and none of the relay flows can be added to SQ_i. Probability of this case is given as:

$$P(a,0,m,n) = 1 - \sum_{i=1}^{n} P(a,i,m,n) \tag{44}$$

$$= 1 - \widetilde{\mathcal{P}}(a,m) \sum_{i=1}^{n} \mathcal{P}'((i,n)|(a,m)) \tag{45}$$

Thus, in the case of even numbered slots, where direct flows are scheduled followed by relay flows, expected number of concurrent transmissions $E_e[C]$ is given by:

$$E_e[C] = \sum_{a=1}^{m}\sum_{b=1}^{n}(a+b)\widetilde{\mathcal{P}}(a,m)\mathcal{P}'((b,n)|(a,m)) \tag{46}$$

$$= \sum_{a=1}^{m}\sum_{b=1}^{n}(a+b)P(a,b,m,n) \tag{47}$$

Similarly, for odd numbered slots, where relay flows are scheduled followed by direct flows, expected number of concurrent transmissions $E_o[C]$ is given by:

$$E_o[C] = \sum_{a=1}^{m}\sum_{b=1}^{n}(b+a)\widetilde{\mathcal{P}}(b,n)\mathcal{P}'((a,m)|(b,n)) \tag{48}$$

$$= \sum_{a=1}^{m}\sum_{b=1}^{n}(b+a)P(b,a,n,m) \tag{49}$$

Hence, the expected number of concurrent flows in a slot is given by:

$$\mathcal{E}[C] = \frac{E_e[C] + E_o[C]}{2} \tag{50}$$

6. Performance evaluation

In this section, we evaluate the performance of our proposed scheme under various system parameters. We perform simulation in Java environment by considering the system model as discussed in Section 2. In simulations, we consider a random distribution of FBSs and relay FBSs within the coverage area of an MiBS of radius R_ψ meters. The value of R_ψ is considered to be equal to d_{mm}, which is beamwidth dependent. The MiBS is considered to be located at the center of the coverage area. All the FBSs are equipped with an electronically steerable directional antenna and use the hybrid beamforming technique. The MiBS is equipped with multiple directional antennas with a fixed boresight beamforming to its corresponding sector. Each MiBS antenna provides the coverage exclusively to its sector without interfering with the transmission from other antennas of MiBS. The number of FBSs per time slot requesting for data transmission are varied from 1 to 50 which consists of both direct and relay communication requests. To obtain each data point we have taken the average of 25 000 different simulation instances. We consider the protocol described in Section 2.5 in our simulations for mode selection, relay selection, and flow scheduling. The detailed simulation parameters are given in Table 1.

We investigate the performance of our proposed scheme in two different scenarios, viz. single FBS and multiple FBSs scenario. All the FBSs are considered to transmit with maximum transmission power P_t in both the scenarios. We compare our proposed scheme with fixed relay probing scheme.

In the fixed relay probing scheme, FBSs probe a fixed number of relays and select the best one among the probed relays. In order to ensure the fixed number of relays probe, we allocate the fixed number of time slots for probing in the probing phase, given by N. We consider two different values for N i.e., 100 and 200. As stated in Section 1 each relay probe may require two independent time slots, one for the source–relay probe and other for the relay–destination probe. In order to perform a fair comparison, in the fixed relay probing scheme also first time slot is allocated for probing for direct mode communication and the following time slots for relay mode probing.

Table 1
Simulation Parameters.

Parameter	Value
Number of FBSs requests (F)	1–50
Number of idle FBSs ($\|Y\|$)	1000
Maximum number of probes (N_{max})	1000
Uplink bandwidth (W)	1.8 GHz
Carrier frequency (f)	60 GHz
MiBS transmit power	30 dBm
FBS transmit power (P_t)	23 dBm
Single model parameter (n)	2.0
Standard deviation (X_σ)	2.9 dB
Additive White Gaussian Noise (AWGN) (σ^2)	−134 dBm/MHz
Pilot time (T_p)	10^{-4} s
Data transmission duration (T)	1 s
Radiation efficiency of FBS (η)	0.8
Average blockage loss (b_{loss})	150 dB
Sector level beamwidth ($\psi_i^t = \psi_i^r$)	2π

In the fixed relay probing scheme, FBSs perform a fixed number of probes irrespective of blockages, backhaul link quality, and terrain conditions. However, our proposed scheme adopts to these conditions by changing the number of probes accordingly.

In Figs. 8(a), 8(c), 8(e), and 8(g), we analyze the variation in throughput for single FBS scenario by varying spectral efficiency threshold (γ). Figs. 8(a) and 8(e) show the performance for beamwidths $\theta = 15°$ and $\theta = 45°$, respectively, under three different link blockage probabilities between FBSs ($p = 0.5$, $p = 0.7$, and, $p = 0.9$) using $p' = 0.5$. Here, p is the probability that link between FBSs is blocked and p' is the probability that link between FBS and MiBS is blocked. The main reason for considering p and p' to be different is to make them independent of each other and to have a better study. The p' is responsible for changing the mode of communication. Smaller the value p' more the chances an FBS will choose the direct mode of communication. On the other hand, the impact of p is on the number of probes. Higher the value of p more number of relays need to be probed in order to satisfy a particular spectral efficiency threshold. From the figures, it can be clearly seen that the throughput initially increases on increasing the spectral efficiency threshold, attains maximum value, and then starts decreasing. In other words, for all the different values of p, there exists an optimal spectral efficiency threshold that maximizes the throughput. We found similar observations for $p' = 0.7$ as shown in Figs. 8(c) and 8(g) for both the values of beamwidths. We select the optimal spectral efficiency threshold for which the throughput is maximum and use it as a heuristic for stopping rule in multi FBSs scenario.

For both the values of beamwidth ($\theta = 15°$ and $\theta = 45°$), it can be noticed from the figures that higher the blockage probability, the smaller the optimal stopping threshold, and lower will be the throughput. This is because more number of relays are probed for relay selection in order to satisfy the spectral efficiency threshold. Moreover, it can be seen that when the spectral efficiency threshold becomes large, a lot of time slots are spent in relay probing. This explains why for the same beamwidth, the gap between the curve with $p = 0.5$, $p = 0.7$, and $p = 0.9$ reduces as the spectral efficiency threshold becomes large.

In Figs. 8(b), 8(d), 8(f), and 8(h), we compare the performance in terms of the number of probes on varying spectral efficiency threshold under three different values of p for $\theta = 15°$ and $\theta = 45°$. From the figures, it can be seen that the number of probes increases on increasing the spectral efficiency threshold for all the values of p. This is because more number of relays are required to be probed in order to satisfy the higher value of spectral efficiency threshold. We can also note that with higher value of p, more number of links are blocked and thus, more number of relays are needed to be probed to satisfy the

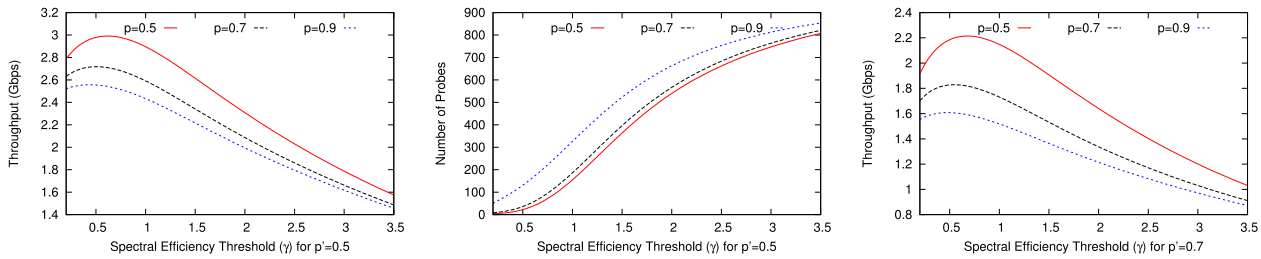

(a) Throughput vs. Spectral Efficiency Threshold for p'=0.5 using Beamwidth $\theta = 15^o$ (b) Number of Probes vs. Spectral Efficiency Threshold for p'=0.5 using Beamwidth $\theta = 15^o$ (c) Throughput vs. Spectral Efficiency Threshold for p'=0.7 using Beamwidth $\theta = 15^o$

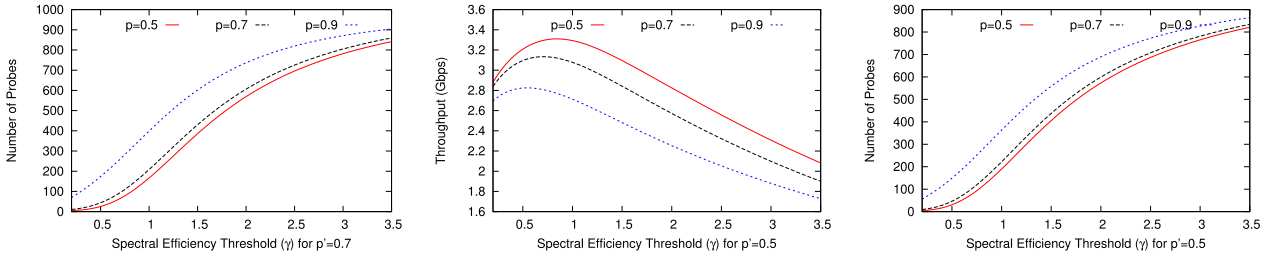

(d) Number of Probes vs. Spectral Efficiency Threshold for p'=0.7 using Beamwidth $\theta = 15^o$ (e) Throughput vs. Spectral Efficiency Threshold for p'=0.5 using Beamwidth $\theta = 45^o$ (f) Number of Probes vs. Spectral Efficiency Threshold for p'=0.5 using Beamwidth $\theta = 45^o$

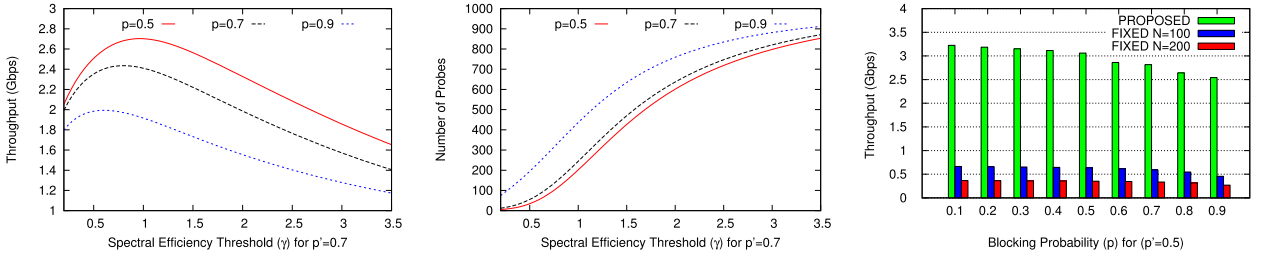

(g) Throughput vs. Spectral Efficiency Threshold for p'=0.7 using Beamwidth $\theta = 45^o$ (h) Number of Probes vs. Spectral Efficiency Threshold for p'=0.7 using Beamwidth $\theta = 45^o$ (i) Throughput vs. Blocking Probability for $p' = 0.5$ for Beamwidth $\theta = 15^o$

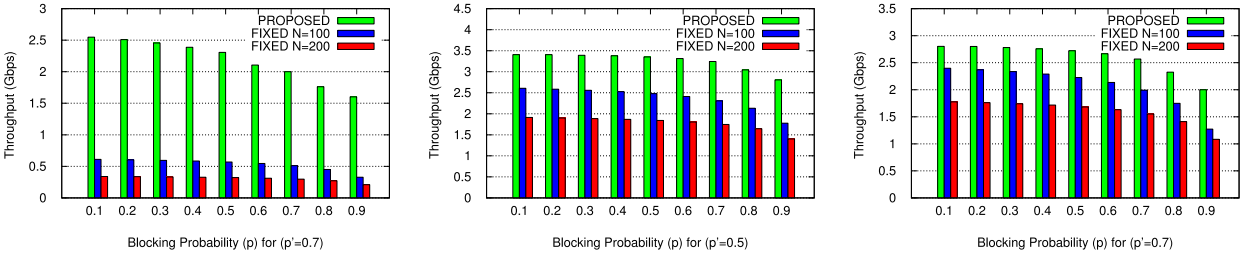

(j) Throughput vs. Blocking Probability for $p' = 0.7$ for Beamwidth $\theta = 15^o$ (k) Throughput vs. Blocking Probability for $p' = 0.5$ for Beamwidth $\theta = 45^o$ (l) Throughput vs. Blocking Probability for $p' = 0.5$ for Beamwidth $\theta = 45^o$

Fig. 8. Variation of throughput vs. spectral efficiency threshold, variation of number of probes vs. spectral efficiency threshold, and variation of throughput vs. blocking probability for fixed relay probing and proposed scheme under single FBS scenario.

spectral efficiency threshold. However, in both the curves, it can be seen that when the spectral efficiency threshold becomes very large the gap between the curve with $p = 0.5$, $p = 0.7$, and $p = 0.9$ reduces as the maximum number of probes are bounded by 1000.

We examine the throughput performance for single FBS scenario on varying blockage probability in Figs. 8(i), 8(j), 8(k), and 8(l). Our proposed scheme outperforms the fixed probing scheme for all the different values of blockage probability p and p'. In both the schemes, fixed relay probing and proposed, throughput decreases with increase in blockage probability. The reason for the decrease in the throughput in the case of fixed relay probing is because of increase in the number of blockages in the environment, which in turns affect the link quality and finally affect the throughput. On the other hand, same reason holds for the proposed scheme also but the proposed scheme uses optimal spectral efficiency threshold as a stopping criterion in order to maximize throughput. Hence, it stops appropriately and performs an optimal number of probes. In case of a fixed probing scheme, number of probes allowed are fixed irrespective of the blockage probabilities. Hence, FBSs may not end up with finding the suitable relay or may perform extra probes which affect the final throughput.

Considering Figs. 8(a) and 8(b), the spectral efficiency threshold at which the throughput is maximum is taken as an optimal spectral

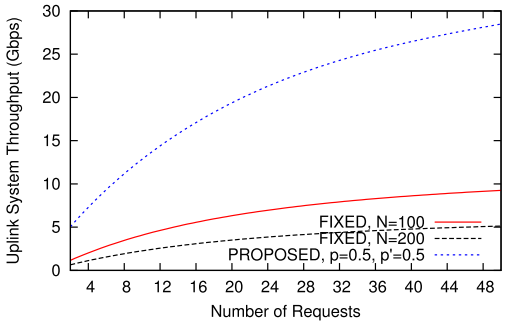

(a) Throughput vs. Number of Requests for ($p = 0.5$, $p' = 0.5$) using Beamwidth $\theta = 15^o$

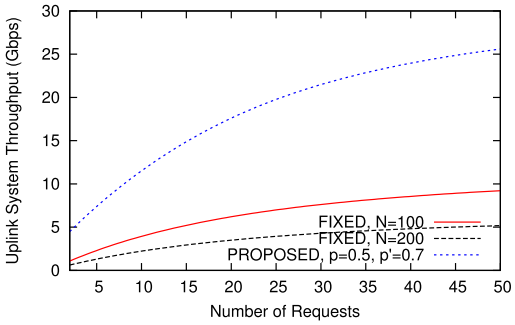

(b) Throughput vs. Number of Requests for ($p = 0.5$, $p' = 0.7$) using Beamwidth $\theta = 15^o$

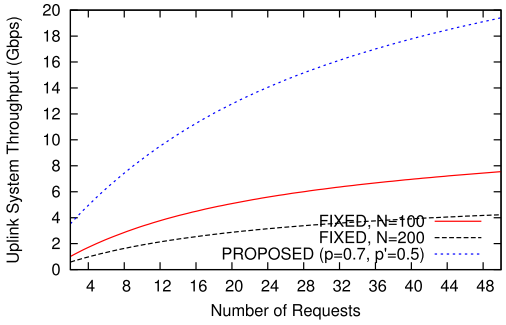

(c) Throughput vs. Number of Requests for ($p = 0.7$, $p' = 0.5$) using Beamwidth $\theta = 15^o$

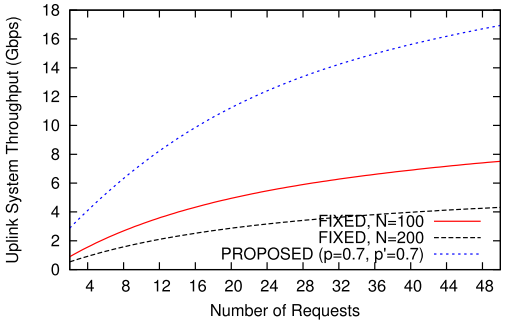

(d) Throughput vs. Number of Requests for ($p = 0.7$, $p' = 0.7$) using Beamwidth $\theta = 15^o$

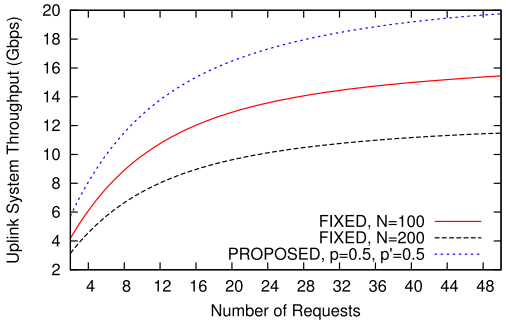

(e) Throughput vs. Number of Requests for ($p = 0.5$, $p' = 0.5$) using Beamwidth $\theta = 45^o$

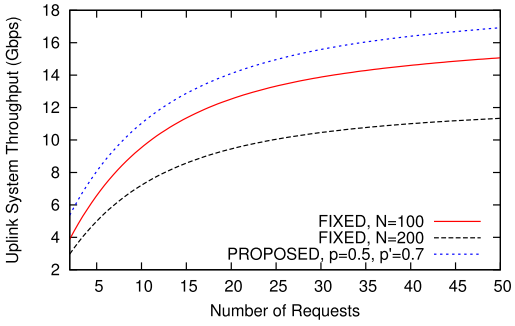

(f) Throughput vs. Number of Requests for ($p = 0.5$, $p' = 0.7$) using Beamwidth $\theta = 45^o$

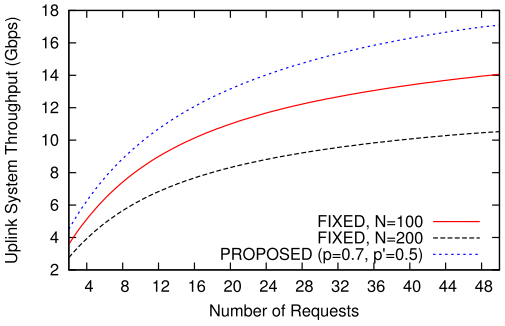

(g) Throughput vs. Number of Requests for ($p = 0.7$, $p' = 0.5$) using Beamwidth $\theta = 45^o$

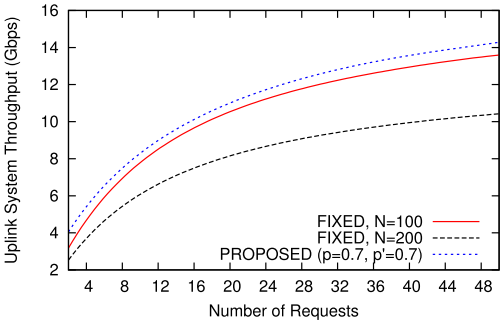

(h) Throughput vs. Number of Requests for ($p = 0.7$, $p' = 0.7$) using Beamwidth $\theta = 45^o$

Fig. 9. Variation of uplink system throughput vs. number of requests for fixed relay probing and proposed scheme under multi FBSs scenario.

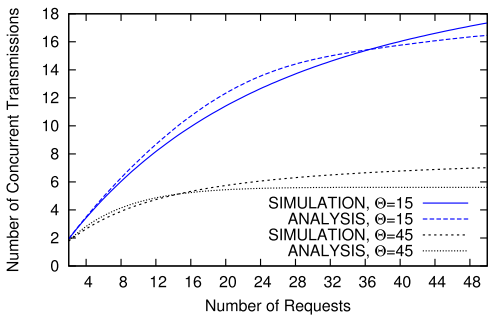

Fig. 10. Number of concurrent transmissions vs. number of requests in multiple FBS transmission scenario using ($p = 0.5, p' = 0.5$) for both analytical and simulation results.

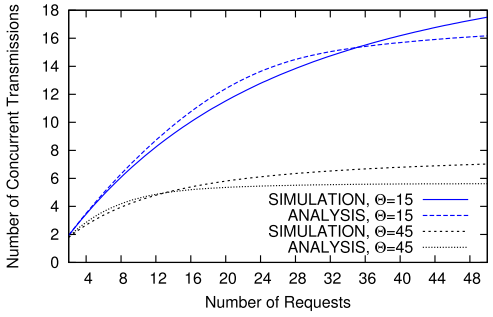

Fig. 11. Number of concurrent transmissions vs. number of requests in multiple FBS transmission scenario using ($p = 0.7, p' = 0.7$) for both analytical and simulation results.

efficiency threshold, and the number of probes corresponds to this threshold is taken as the bound (N^*) for the multi FBSs scenario. Both these parameter values are learned periodically based on blockages in the environment and sent from MiBS to all FBSs.

In all the sub-figures of Fig. 9, we investigate the performance of uplink system throughput by varying number of link requests for fixed relay probing with $N = 100$ and $N = 200$ and the proposed scheme for different combinations of blockage probabilities and beamwidths. For a fair comparison between these two schemes, we consider the same concurrent backhaul link scheduling algorithm as discussed in Section 4.4. From the sub-figures, we observe that the number of concurrent transmissions increases on increasing the number of FBSs requests and thus the uplink system throughput increases. However, it is important to observe that after a certain number of FBS requests throughput growth becomes slow as the maximum spatial reuse is reached (i.e., the number of concurrent transmissions tends to reach to its maximum value). It can be observed from the sub-figures for all the values of blockage probabilities and beamwidths, our scheme performs better than the fixed probing scheme.

The fixed probing scheme uses the fixed number of probes for all the FBSs requested in the same frame as a stopping rule. The disadvantage of the fixed probing scheme is that it does not account for the density of the blockages (i.e, blockage probability). Hence, it may add unnecessary probing overhead or may stop probing too early. However, in the case of the proposed scheme, we use optimal stopping spectral efficiency threshold and a maximum number of probes bound (N_m^*) which depends upon different combinations of blockage probabilities and beamwidths. Stopping spectral efficiency threshold used from the single FBS scenario is one which provides the maximum throughput for the particular combination and helps in maximizing the uplink system throughput. We also observe that for a fixed value of beamwidth in both the schemes, throughput performance is better for lower blockage probability ($p = 0.5$) than that of the higher blockage probability ($p = 0.7$). This is because increasing the blockage probability will increase the number of blockages in the environment and affect the link quality. In the case of proposed scheme one more reason is higher the blockage probability, more the number of probes need to be performed (to find appropriate FBS-FBS(Relay)-MiBS link), which in turn increases the probing phase overhead and reduces the effective uplink system throughput. However, because of usage of optimal stopping rule and a maximum number of probes bound (N_m^*), the proposed scheme maintains the best tradeoff between the throughput gain obtained from searching a better relay and the throughput loss due to the higher relay probing overhead.

We analyze the number of concurrent flow transmissions possible by varying the number of link requests in Figs. 10 and 11. We have plotted the data points obtained from both analysis as well as simulations for the proposed scheme. Similar results are obtained for fixed relay probing scheme also as we consider the same scheduling algorithm, and both schemes request MiBS with almost same number of direct and relay based flow requests. Figs. 10 and 11 validate our simulations and analysis. From the figures, we observe that the simulations and analysis results show the same trends. We also observe that the number of concurrent flow transmissions increases on increasing the FBSs requests, as the MiBS finds more number of non-interfering candidates that can be scheduled concurrently. However, after a certain number of FBSs requests, the growth in the number of concurrent transmissions becomes slow as maximum spatial reuse is reached. Irrespective of the similar number of concurrent transmissions for all the different values of link request in both the schemes, our proposed scheme shows superior uplink system throughput performance compared to fixed relay probing scheme as shown in Fig. 9 because of the use of optimal stopping rule criteria and bound on maximum number of probes in the probing phase.

In Figs. 10 and 11, we also observe that for a lower value of beamwidth we obtain a higher number of concurrent transmissions compared to the higher value of beamwidth. This is because higher value of beamwidth covers a larger area and hence, decreases the spatial reuse.

Our proposed algorithm also helps to improve energy efficiency significantly. The energy efficiency of the network is measured generally using Energy Consumption Rating (ECR), which is the ratio of the total energy consumption by FBSs to the total system capacity. It is important to note here that the lower the value of ECR, the more energy-efficient the system will be and vice versa. One way to achieve the lower value of ECR is by improving the system capacity (System Throughput). As our proposed algorithm improves the system throughput significantly and in turns the energy efficiency.

7. Conclusion

High-frequency mmWave signals are highly susceptible to blockages and thus suffer a high attenuation in signal strength when passed through these obstacles. In order to solve this problem, a joint distributed mode selection and relay selection scheme is proposed in this paper for mmWave based FBSs network. In contrast to the existing research which is mainly focussed on FBSs using broadband connection based backhaul which can provide capacity up to only tens of Mbps, in this paper, we focussed on mode selection, relay probing, and efficient backhaul scheduling for FBSs using mmWave based backhaul. We studied a more practical and realistic scenario in scheduling the backhaul links for FBSs by explicitly considering the relay probing and beam-alignment overhead. Our proposed solution determines better mode of data transfer and selects the best relay in the case of relay mode selection. We derived the stopping rule conditions for single FBS and multiple FBSs scenarios, and also derived the heuristics for concurrent backhaul link scheduling decisions. In order to validate our proposed scheduling scheme we also derived an expression for calculating the expected number of concurrent transmissions. Finally, we have shown the superiority of our proposed mode selection and relay probing scheme over fixed relay probing under various system

parameters. Future extension of this work can analytically evaluate the proposed mode selection and relay probing scheme. Also, conducting packet delay analysis for the proposed scheduling scheme using an appropriate queuing model would be an interesting future work.

Declaration of competing interest

The authors declare that they have no known competing financial interests or personal relationships that could have appeared to influence the work reported in this paper.

Acknowledgment

This research work was supported by the Department of Science and Technology, New Delhi, India Grant Number: SB/S2/JCB-008/2016.

References

[1] N. Alliance, 5G white paper, Next generation mobile networks, white paper.
[2] D. Choudhury, 5G wireless and millimeter wave technology evolution: An overview, in: Proceedings of the IEEE MTT-S International Microwave Symposium, 2015, pp. 1–4.
[3] V. Chandrasekhar, J.G. Andrews, A. Gatherer, Femtocell networks: A survey, IEEE Commun. Mag. 46 (9) (2008) 59–67.
[4] F.S. Chu, C.H. Lee, K.C. Chen, Backhaul-constrained resource optimization for distributed femtocell interference mitigation, in: Proceedings of the IEEE Wireless Communications and Networking Conference (WCNC), 2014, pp. 1485–1489.
[5] I. Hwang, B. Song, S. Soliman, A holistic view on hyper-dense heterogeneous and small cell networks, IEEE Commun. Mag. 51 (6) (2013) 20–27.
[6] A. Chaudhari, C.S.R. Murthy, Femto-to-Femto (F2F) communication: The next evolution step in 5G wireless backhauling, in: Proceedings of the IEEE 15th International Symposium on Modeling and Optimization in Mobile, Ad Hoc, and Wireless Networks (WiOpt), 2017, pp. 1–8.
[7] J. Choi, V. Va, N. Gonzalez-Prelcic, R. Daniels, C.R. Bhat, R.W. Heath, Millimeter-wave vehicular communication to support massive automotive sensing, IEEE Commun. Mag. 54 (12) (2016) 160–167.
[8] H. Song, X. Fang, Y. Fang, Millimeter-wave network architectures for future high-speed railway communications: Challenges and solutions, IEEE Wirel. Commun. 23 (6) (2016) 114–122.
[9] Y. Niu, Y. Li, D. Jin, L. Su, A.V. Vasilakos, A survey of millimeter wave communications (mmwave) for 5G: opportunities and challenges, Wirel. Netw. 21 (8) (2015) 2657–2676.
[10] S. Rangan, T.S. Rappaport, E. Erkip, Millimeter-wave cellular wireless networks: Potentials and challenges, Proc. IEEE 102 (3) (2014) 366–385.
[11] Z. Pi, F. Khan, An introduction to millimeter-wave mobile broadband systems, IEEE Commun. Mag. 49 (6) (2011).
[12] P. Pietraski, D. Britz, A. Roy, R. Pragada, G. Charlton, Millimeter wave and terahertz communications: Feasibility and challenges, ZTE Commun. 10 (4) (2012) 3–12.
[13] J.S. Lu, D. Steinbach, P. Cabrol, P. Pietraski, Modeling human blockers in millimeter wave radio links, ZTE Commun. 10 (4) (2012) 23–28.
[14] J. Chen, J. Liu, P. Wang, J. Zhang, Backhaul constraint-based cooperative interference management for in-building dense femtocell networks, in: Proceedings of the IEEE Vehicular Technology Conference (VTC Fall), 2012, pp. 1–5.
[15] R. Thakur, S.N. Swain, C.S.R. Murthy, An energy efficient cell selection framework for femtocell networks with limited backhaul link capacity, IEEE Syst. J. PP (99) (2017) 1–12.
[16] T. Baykas, C.-S. Sum, Z. Lan, J. Wang, M.A. Rahman, H. Harada, S. Kato, IEEE 802.15.3c: the first IEEE wireless standard for data rates over 1 Gb/s, IEEE Commun. Mag. 49 (7) (2011).
[17] Draft standard for information technology-telecommunications and information exchange be- tween systems-local and metropolitan area networks-specific requirements-part 11: Wireless LAN Medium Access Control (MAC) and physical layer (PHY) specifications-amendment 4: Enhancements for very high throughput in the 60 GHz band (2012).
[18] H. Rate, GHz PHY, MAC and HDMI PAL (2008.
[19] L.X. Cai, L. Cai, X. Shen, J.W. Mark, Rex: A randomized EXclusive region based scheduling scheme for mmwave WPANs with directional antenna, IEEE Trans. Wirel. Commun. 9 (1) (2010) 113–121.
[20] C.-S. Sum, Z. Lan, M.A. Rahman, J. Wang, T. Baykas, R. Funada, H. Harada, S. Kato, A multi-Gbps millimeter-wave WPAN system based on STDMA with heuristic scheduling, in: Proceedings of the IEEE Global Telecommunications Conference GLOBECOM, 2009, pp. 1–6.
[21] C.-S. Sum, Z. Lan, R. Funada, J. Wang, T. Baykas, M. Rahman, H. Harada, Virtual time-slot allocation scheme for throughput enhancement in a millimeter-wave multi-Gbps WPAN system, IEEE J. Sel. Areas Commun. 27 (8) (2009).
[22] W. ur Rehman, J. Han, C. Yang, M. Ahmed, X. Tao, On scheduling algorithm for device-to-device communication in 60 GHz networks, in: Proceedings of the IEEE Wireless Communications and Networking Conference (WCNC), 2014, pp. 2474–2479.
[23] J. Qiao, L.X. Cai, X. Shen, J.W. Mark, STDMA-based scheduling algorithm for concurrent transmissions in directional millimeter wave networks, in: Proceedings of the IEEE International Conference on Communications (ICC), 2012, pp. 5221–5225.
[24] Z. He, S. Mao, A decomposition principle for link and relay selection in dual-hop 60 GHz networks, in: Proceedings of the IEEE International Conference on Computer Communications (INFOCOM), 2016, pp. 1–9.
[25] J. Qiao, X.S. Shen, J.W. Mark, Q. Shen, Y. He, L. Lei, Enabling Device-to-Device communications in millimeter-wave 5G cellular networks, IEEE Commun. Mag. 53 (1) (2015) 209–215.
[26] G. Tran, R. Santos, H. Ogawa, M. Nakamura, K. Sakaguchi, A. Kassler, Context-based dynamic meshed backhaul construction for 5G heterogeneous networks, J. Sens. Actuator Netw. 7 (4) (2018) 43.
[27] H. Ogawa, G.K. Tran, K. Sakaguchi, T. Haustein, Traffic adaptive formation of mmWave meshed backhaul networks, in: Proceedings of the IEEE International Conference on Communications Workshops (ICC Workshops), 2017, pp. 185–191.
[28] A. Mesodiakaki, E. Zola, R. Santos, A. Kassler, Optimal user association, backhaul routing and switching off in 5G heterogeneous networks with mesh millimeter wave backhaul links, Ad hoc Netw. 78 (2018) 99–114.
[29] N. Wei, X. Lin, Z. Zhang, Optimal relay probing in millimeter-wave cellular systems with Device-to-Device relaying, IEEE Trans. Veh. Technol. 65 (12) (2016) 10218–10222.
[30] M. Rebato, M. Mezzavilla, S. Rangan, M. Zorzi, Resource sharing in 5G mmwave cellular networks, in: Proceedings of the IEEE Conference on Computer Communications Workshops (INFOCOM WKSHPS), 2016, pp. 271–276.
[31] H. Shokri-Ghadikolaei, L. Gkatzikis, C. Fischione, Beam-searching and transmission scheduling in millimeter wave communications, in: Proceedings of the IEEE International Conference on Communications (ICC), 2015, pp. 1292–1297.
[32] Y. Tsang, A.S. Poon, S. Addepalli, Coding the beams: Improving beamforming training in mmwave communication system, in: Proceedings of the IEEE Global Telecommunications Conference (GLOBECOM), 2011, pp. 1–6.
[33] R. Ramanathan, On the performance of ad hoc networks with beamforming antennas, in: Proceedings of the 2nd ACM International Symposium on Mobile Ad Hoc Networking & Computing (MobiHoc), 2001, pp. 95–105.
[34] S. Sun, T.S. Rappaport, S. Rangan, T.A. Thomas, A. Ghosh, I.Z. Kovacs, I. Rodriguez, O. Koymen, A. Partyka, J. Jarvelainen, Propagation path loss models for 5G urban micro- and macro-cellular scenarios, in: Proceedings of the IEEE 83rd Vehicular Technology Conference (VTC Spring), 2016, pp. 1–6.
[35] G. Kramer, M. Gastpar, P. Gupta, Cooperative strategies and capacity theorems for relay networks, IEEE Trans. Inf. Theory 51 (9) (2005) 3037–3063.
[36] C.E. Shannon, A mathematical theory of communication, ACM SIGMOBILE Mob. Comput. Commun. Rev. 5 (1) (2001) 3–55.